AGU ADVANCING EARTH AND SPACE SCIENCE

Water Resources Research

RESEARCH ARTICLE
10.1029/2022WR031954

A Vine Copula-Based Polynomial Chaos Framework for Improving Multi-Model Hydroclimatic Projections at a Multi-Decadal Convection-Permitting Scale

Boen Zhang[1], Shuo Wang[1,2], Yamin Qing[1], Jinxin Zhu[3], Dagang Wang[3], and Jiafeng Liu[4]

[1]Department of Land Surveying and Geo-Informatics, Research Institute for Land and Space, The Hong Kong Polytechnic University, Hong Kong, China, [2]Shenzhen Research Institute, The Hong Kong Polytechnic University, Shenzhen, China, [3]School of Geography and Planning, Sun Yat-Sen University, Guangzhou, China, [4]China Aero Geophysical Survey and Remote Sensing Center, Beijing, China

Abstract Physically based hydrologic models have been extensively used for hydroclimatic projections, but key challenges remain owing to the heavy computational burden and structural variability of physically based models. In this study, we develop a vine copula-based polynomial chaos framework for improving multi-model projections of hydroclimatic regimes at a convection-permitting scale over the Dongjiang River Basin located in South China. Specifically, a deep neural network (DNN)-based polynomial chaos expansion (PCE) is developed to significantly improve the efficiency of probabilistic hydrologic predictions. A vine copula multi-model ensemble approach is also proposed to robustly combine hydrologic predictions generated from multiple DNN-based PCEs to improve reliability and accuracy. To assess regional hydrologic responses to changing climate, multi-decadal nested-grid climate projections over the Guangdong-Hong Kong-Macao Greater Bay Area (GBA) are developed using the convection-permitting Weather Research and Forecasting (WRF) model with 4-km horizontal grid spacing. Our findings reveal that the DNN-based PCEs achieve comparable performance to the physically based hydrologic predictions with an extremely low computational cost. The vine copula multi-model ensemble approach outperforms the Bayesian model averaging (BMA) by generating more accurate and reliable hydrologic predictions. The developed framework and physical models also lead to consistent projections of future changes in streamflow regimes. Our findings reveal that the projected increases in the frequency and intensity of extreme precipitation can lead to substantial increases in flood magnitudes, but the increases may not be obvious for river basins affected by multiple reservoirs.

Key Points:

- A deep neural network-based polynomial chaos expansion was developed to improve the efficiency of probabilistic hydrologic prediction
- A vine copula multi-model ensemble approach was proposed to improve the accuracy of ensemble hydrologic prediction
- Convection-permitting climate simulations were conducted for improving the reliability of assessing regional hydrologic responses to changing climate

Supporting Information:

Supporting Information may be found in the online version of this article.

Correspondence to:

S. Wang,
shuo.s.wang@polyu.edu.hk

Citation:

Zhang, B., Wang, S., Qing, Y., Zhu, J., Wang, D., & Liu, J. (2022). A vine copula-based polynomial chaos framework for improving multi-model hydroclimatic projections at a multi-decadal convection-permitting scale. *Water Resources Research*, *58*, e2022WR031954. https://doi.org/10.1029/2022WR031954

Received 8 JAN 2022
Accepted 13 MAY 2022

Author Contributions:

Conceptualization: Shuo Wang
Data curation: Boen Zhang, Yamin Qing
Formal analysis: Boen Zhang
Funding acquisition: Shuo Wang
Investigation: Shuo Wang
Methodology: Boen Zhang, Shuo Wang
Project Administration: Shuo Wang
Resources: Shuo Wang, Jinxin Zhu, Dagang Wang, Jiafeng Liu
Software: Boen Zhang, Shuo Wang, Yamin Qing
Supervision: Shuo Wang
Validation: Boen Zhang, Shuo Wang, Yamin Qing
Visualization: Boen Zhang
Writing – original draft: Boen Zhang

1. Introduction

Understanding regional hydrologic responses to changing climate is vital for effective water resources planning and risk assessment of water-related hazards (Gudmundsson et al., 2021; B. Zhang et al., 2021; Zscheischler et al., 2020). Thus, improving hydroclimatic projections plays a crucial role in supporting decision-making by policymakers and stakeholders, also fostering actions to reduce potential risks and impacts on water resources under current and future climate conditions. Hydrologic prediction systems driven by regional climate models have been routinely used to assess future changes in catchment-scale hydrologic regimes in a warming climate, which has attracted widespread attention from the hydroclimate community in recent years (Anghileri et al., 2016; Kurkute et al., 2020; Musselman et al., 2018; You & Wang, 2021).

Physically based hydrologic models are an essential tool for assessing hydrologic regimes in response to climate change, but they are subject to a variety of uncertainties, such as those in model parameters, thereby resulting in inevitable uncertainties in hydroclimatic projections (Qing et al., 2022; Tran et al., 2020; B. Zhang et al., 2019; S. Wang et al., 2018; S. Wang & Wang, 2019). Over the past decade, tremendous efforts have been devoted to addressing uncertainties in hydrologic model parameters (Laloy et al., 2013; H. Li & Zhang, 2007; Moradkhani et al., 2005; Vrugt, 2016). Monte Carlo (MC) simulation is one of the most widely used uncertainty analysis techniques but is quite time-consuming since a great number of model simulations are required for accurate estimates (Maina & Siirila-Woodburn, 2020; Tran et al., 2020; J. Zhang et al., 2020). To overcome this problem, a simpler representation of physical models has been investigated through various surrogate techniques (Bass & Bedient, 2018; Razavi et al., 2012; Viana et al., 2021), among which polynomial chaos expansion (PCE) has gained popularity due to its ability to efficiently estimate the effects of parameter uncertainty on model outputs (Hu et al., 2019; Man et al., 2019; H. Wang et al., 2020). PCE acts as a computationally efficient surrogate model

Writing – review & editing: Shuo Wang, Jinxin Zhu, Dagang Wang, Jiafeng Liu

in which the variability of the output is represented by the ensemble of the expansion coefficient. However, one of the main limitations of PCE is that the time-variant PCE coefficients are estimated based on observations at each time step for a dynamical system, indicating that PCE cannot be used for hydrologic predictions for future periods without observations (Dai et al., 2016; Fan et al., 2016; Liao & Zhang, 2016; Lin & Tartakovsky, 2009; Torre et al., 2019). Little effort has been devoted to improving PCE for implementing future hydrologic predictions. In recent years, deep neural networks (DNNs) have been attracting extensive attention in the hydroclimate community due to their predictive power and portability (Ghaith & Li, 2020). Since the time-dependent PCE coefficients determine the model outputs of interest, adopting DNNs to predict PCE coefficients based on hydroclimate variables generated from climate models can lead to efficient probabilistic hydrologic predictions. It is thus desired to develop a DNN-based PCE framework for improving the efficiency of probabilistic hydrologic predictions without compromising physical representations.

All physically based distributed models are the simplified representation of complex physical processes involved in the hydrologic cycle (Yan et al., 2020). Hydrologic projections generated from a single model inevitably become inaccurate and unreliable due to assumptions in the model conceptualization (W. J.M. Knoben et al., 2020; Krysanova et al., 2017; Melsen et al., 2018). To address this issue, multi-model hydrologic predictions are commonly assembled through various techniques to reduce model structural uncertainty (Bohn et al., 2010; Duan et al., 2007; Kollet et al., 2017; W. Li & Sankarasubramanian, 2012; Madadgar & Moradkhani, 2014; S. Sharma et al., 2019). Bayesian model averaging (BMA) is one of the most widely used approaches to combining an ensemble of hydrologic predictions (Biondi & Todini, 2018; Raftery et al., 2005; Vrugt & Robinson, 2007). BMA builds a weighted average of probability density functions (PDFs) centered on the bias-corrected predictions from a set of individual models (Olson et al., 2016; B. Zhang & Wang, 2021). However, the conditional PDF of each model is commonly assumed to follow a normal or gamma distribution in BMA, which may be invalid for hydrologic variables typically with substantial skewness (Blum et al., 2017; Madadgar & Moradkhani, 2014). The vine copula is a flexible and powerful approach to assessing complex interactions among multiple hydroclimatic variables without an assumption on the type of marginal probability distributions (AghaKouchak et al., 2014; Bevacqua et al., 2017; Gruber & Czado, 2018; Liu et al., 2018; Sadegh et al., 2017; C. Sun et al., 2021). However, little effort has been devoted to using the flexible structures of vine copula for improving the multi-model combination. Therefore, a vine copula-based multi-model ensemble approach is needed to implement a flexible combination of multiple model outputs for improving the accuracy and reliability of ensemble hydrologic predictions.

In addition to hydrologic predictions, high-resolution climate simulations with an acceptable accuracy are equally vital for projecting future changes in catchment-scale hydroclimatic regimes. Unfortunately, existing hydroclimatic projections are often conducted based on regional climate models (RCMs) with a horizontal grid spacing of 10–50 km, which rely on convection parameterization schemes, leading to substantial errors in regional hydroclimatic simulations (Olson et al., 2016; Zhu et al., 2019). The intermodel spread of climate sensitivity primarily arises from the poor representation of convection and related processes in RCMs (Becker & Wing, 2020). To address this issue, convection-permitting climate simulations with explicitly resolve deep convection have attracted increasing attention in recent years, which can provide added values to simulated precipitation which is one of the most important variables influencing hydrologic behavior (Giorgi, 2019; Prein et al., 2017; Qing & Wang, 2021). It is thus necessary to assess hydrologic regimes in response to climate change at a convection-permitting scale.

To address the aforementioned limitations of previous studies, we develop a vine copula-based polynomial chaos framework for robustly improving multi-model projections of hydroclimatic regimes over the Guangdong-Hong Kong-Macao Greater Bay Area (GBA). Specifically, a DNN-based PCE is developed for enabling PCE to efficiently implement probabilistic hydrologic predictions for future periods without hydrologic observations. A vine copula multi-model ensemble approach is proposed to perform a flexible combination of outputs from multiple DNN-based PCE models for improving the accuracy of ensemble hydrologic predictions. Convection-Permitting Weather Research and Forecasting (WRF) simulations are also conducted to further improve the reliability of assessing regional hydrologic response to the changing climate over the Dongjiang River Basin of China's GBA which is highly vulnerable to water-related hazards induced by climate change.

The paper is organized as follows. Section 2 describes the vine copula-based polynomial chaos framework (see Figure 1), models, algorithms, performance metrics, and data sets used in this study. Section 3 presents a thorough analysis and discussion on the evaluation of multi-model stochastic hydrologic predictions and

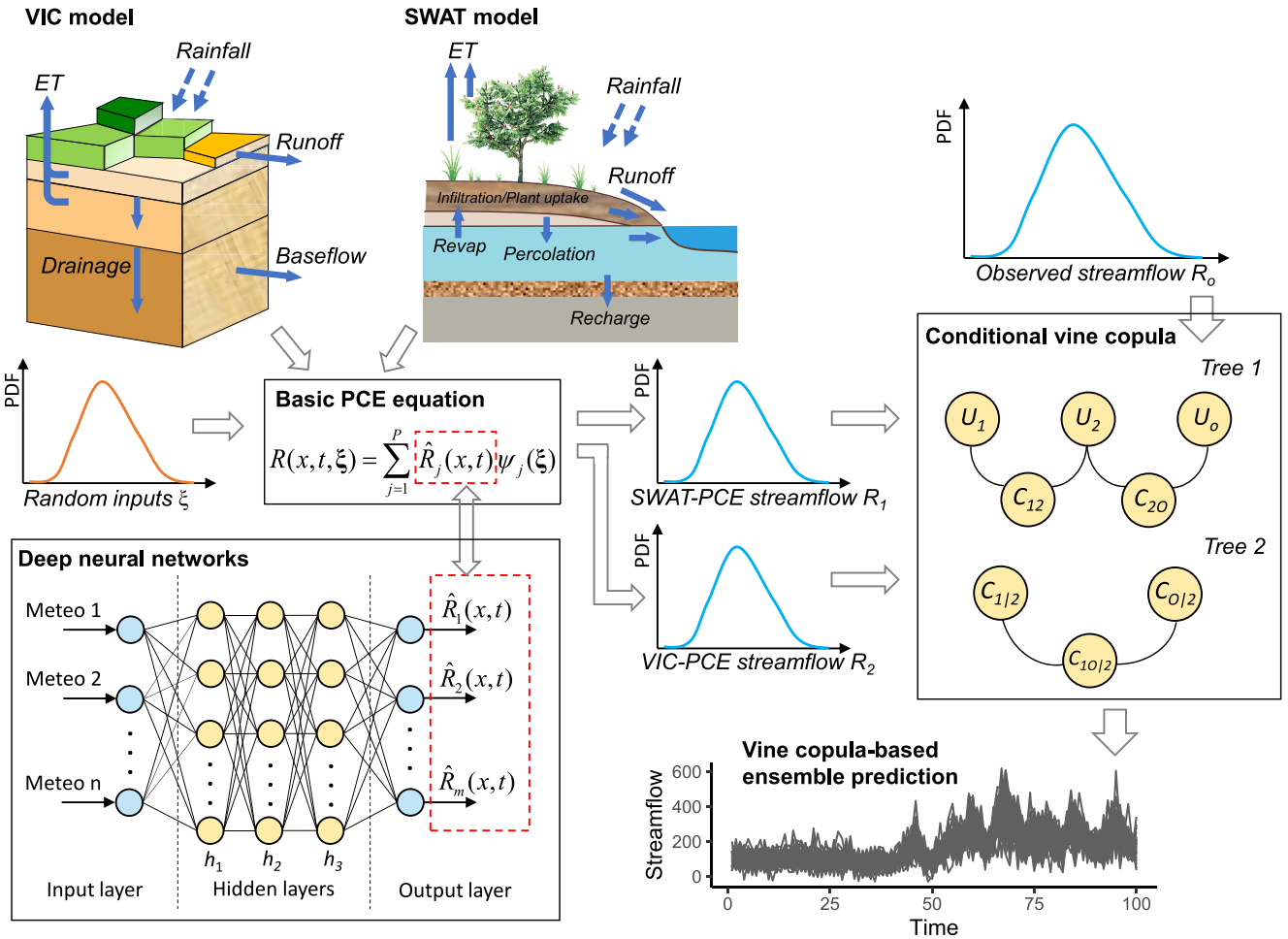

Figure 1. Schematic of the vine copula-based polynomial chaos framework that integrates the deep neural network-based polynomial chaos expansion with the vine copula multi-model ensemble approach. The "Meteo" represents meteorological variables. Soil and water assessment tool (SWAT) and variable infiltration capacity (VIC) hydrologic models are used to develop polynomial chaos expression (PCE)-based surrogate models, in which the PCE coefficients are estimated through deep neural networks (DNNs) for future periods without observations. Model outputs from two DNN-based PCE models are combined through the conditional vine copula to generate ensemble predictions.

convection-permitting climate simulations as well as the projected future changes in hydrologic regimes. Section 4 discusses the results and examines the contribution of PCE-based hydrologic model parameters and structures to the overall uncertainty in streamflow projection. Finally, Section 5 summarizes our study and highlights the main findings.

2. Methods and Data Sources

2.1. Deep Neural Network-Based Polynomial Chaos Expansion (PCE)

A DNN-based PCE is developed in this study for improving probabilistic daily streamflow predictions at two gauging stations located in the Dongjiang River Basin (see Figure 2). To quantify the uncertainty of physically based hydrologic models, model outputs can be numerically approximated based on the concept of PCE, originally proposed by Wiener (1938), as an orthogonal polynomial expression of a predefined random variable ξ by

$$R(t,\xi)=\hat{R}_0(t)+\sum_{i_1=1}^{\infty}\hat{R}_{i_1}(t)\Gamma_1\left(\xi_{i_1}\right)+\sum_{i_1=1}^{\infty}\sum_{i_2=1}^{i_1}\hat{R}_{i_1 i_2}(t)\Gamma_2\left(\xi_{i_1},\xi_{i_2}\right)+\ldots \quad (1)$$

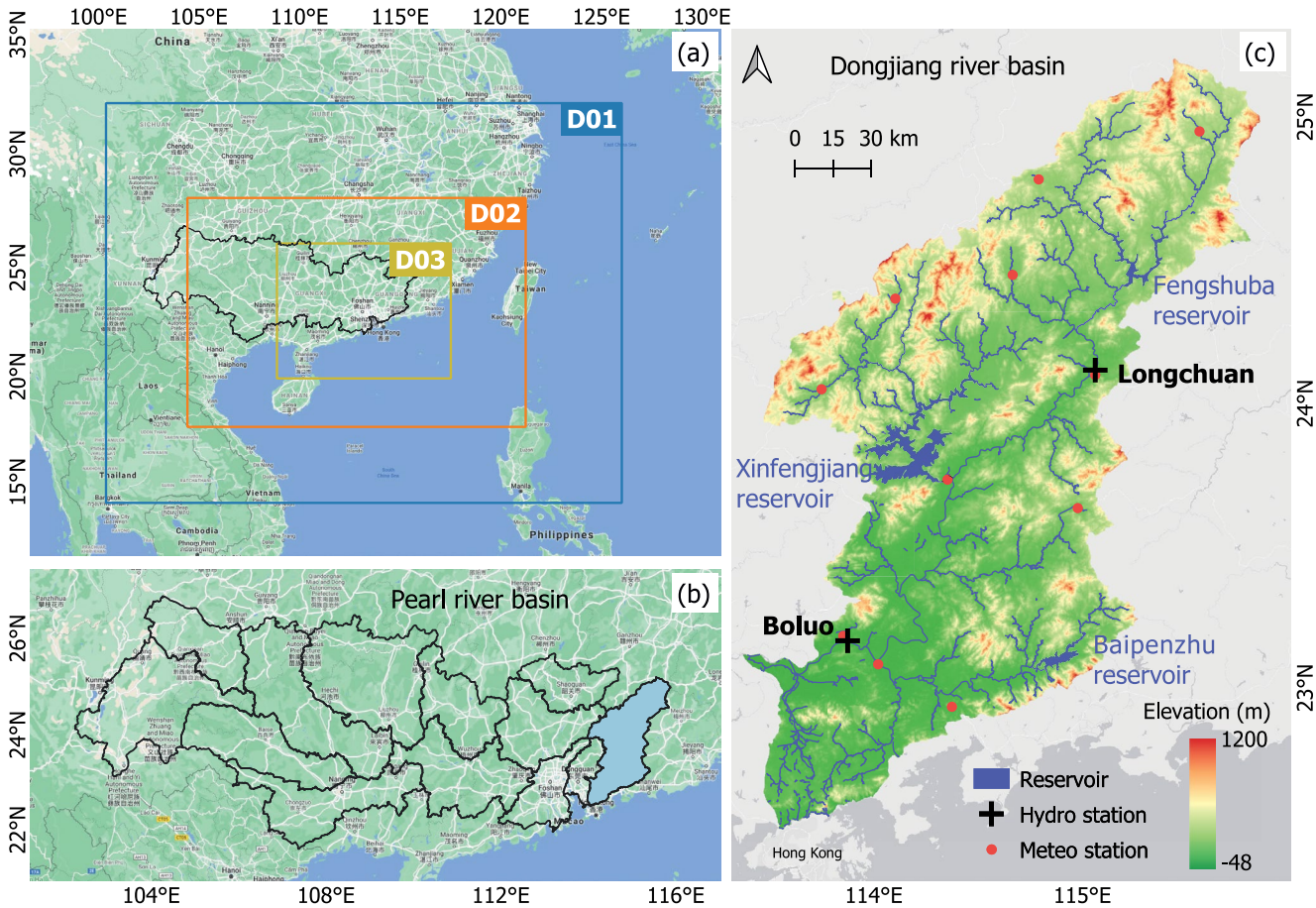

Figure 2. (a) The three nested WRF model domains (D01, D02, and D03) with horizontal grid spacings of 36, 12, and 4 km, respectively. (b) Pearl River Basin and (c) Dongjiang River Basin. WRF = Weather Research and Forecasting.

where $\hat{R}_0(t)$, $\hat{R}_{i_1}(t)$, and $\hat{R}_{i_1 i_2}(t)$ represent the unknown PCE coefficients to be estimated at time t; $R(t, \boldsymbol{\xi})$ represents the model outputs at time t; $\boldsymbol{\xi} = \{\xi_1, \xi_2, \ldots, \xi_N\}^T$ is a vector of standard normal random variables with zero mean and unit variance; $\Gamma_d\left(\xi_{i_1}, \ldots, \xi_{i_d}\right)$ are Hermite polynomials representing the variation of model outputs in the uncertainty space, which can be expressed as

$$\Gamma_d\left(\xi_{i_1}, \ldots, \xi_{i_d}\right) = (-1)^d e^{\frac{1}{2}\xi^T\xi} \frac{\partial^d}{\partial\xi_{i_1}\cdots\partial\xi_{i_d}} e^{-\frac{1}{2}\xi^T\xi} \tag{2}$$

To simplify the polynomial in Equation 1, the output of hydrologic models can be approximated as

$$R(t, \xi) = \sum_{j=0}^{P} \hat{R}_j(t)\psi_j(\xi) \tag{3}$$

where there is a one-to-one correspondence between functions $\Gamma_d(\xi_{i_1},\ldots,\xi_{i_d})$ and $\psi_j(\boldsymbol{\xi})$. P represents the total number of PCE terms, which is a function of the PCE order (d) and the dimensionality N as

$$P = \frac{(N+d)!}{N!d!} \tag{4}$$

A second-order PCE is commonly used in hydrologic simulations and has been demonstrated to generate reliable outputs (Maina & Siirila-Woodburn, 2020; Tran et al., 2020; J. Zhang et al., 2020), which can be written as

$$R(t,\xi) = \hat{R}_0(t) + \sum_{i=1}^{N} \hat{R}_i(t)\xi_i + \sum_{i=1}^{N} \hat{R}_{ii}(t)\left(\xi_i^2 - 1\right) + \sum_{i=1}^{N}\sum_{j=1}^{i-1} \hat{R}_{ij}(t)\xi_i\xi_j \quad (5)$$

The basic idea of a PCE-based surrogate model is to use Equation 5 to construct the relationship between random variables $\boldsymbol{\xi}$ and stochastic outputs R at each time step. Since physically based hydrologic models have a large number of parameters, it is desired to only retain the parameters highly sensitive to the model output (Gonçalves et al., 2016; X. Sun et al., 2018). Sensitivity analysis can thus be performed to select n most sensitive parameters $\boldsymbol{\theta} = \{\theta_1, \theta_2, \ldots, \theta_n\}^T$. $\boldsymbol{\theta}$ is commonly assumed to follow a uniform distribution and can then be transformed from the uniform space into the standard normal space $\boldsymbol{\xi}$ through Equation 6.

$$\xi_i = \sqrt{2}\mathrm{erf}^{-1}\left(\frac{2(\theta_i - a_i)}{b_i - a_i} - 1\right) \quad (6)$$

where $a_i \le \theta_i \le b_i$ represents the range of the ith uncertain parameter (Isukapalli, 1999). The erf^{-1} represents the inverse error function.

The PCE-based hydrologic simulations can be generated if the unknown coefficients $\hat{R}_j(t)$ are accurately estimated. The probabilistic collocation method is commonly used for estimating PCE coefficients, in which model outputs at a set of selected collocation points are approximated as an orthogonal polynomial in terms of random variables. Thus, it is necessary to select a set of collocation points and to obtain the corresponding model simulation results. A standard collocation technique is to specify the collocation points as combinations of the roots of the polynomial of one degree higher than the order of the given PCE. For a two-dimensional second-order PCE, the collocation points are selected from the three roots ($-\sqrt{3}$, 0, and $\sqrt{3}$) of the third-order Hermite polynomial $\mathrm{H}_3(\xi) = \xi^3 - 3\xi$. The available collocation points are (0, 0), ($-\sqrt{3}$, 0), (0, $-\sqrt{3}$), (0, $\sqrt{3}$), ($\sqrt{3}$, 0), ($\sqrt{3}$, $\sqrt{3}$), ($-\sqrt{3}$, $-\sqrt{3}$), ($-\sqrt{3}$, $\sqrt{3}$), and ($\sqrt{3}$, $-\sqrt{3}$). Thus, the model simulations can be performed by specifying parameter values corresponding to the collocation points. However, an N-dimensional PCE of order d has $(d+1)^N$ collocation points but only P unknown coefficients, as shown in Equation 4, indicating that the number of available collocation points increases exponentially as dimension N increases. All the available collocation points are used in the standard collocation technique, which is time-consuming for the high-dimensional PCE. To alleviate the computation burden of the standard collocation technique and to ensure the degree of accuracy, Isukapalli (1999) proposed a regression-based collocation method, which requires fewer number of sample points to effectively capture the behavior of hydrologic models. The regression-based method was used in this study to estimate the unknown coefficients in PCE.

The PCE coefficients are time-variant and are estimated based on hydrologic observations, indicating that the coefficients are not available for future periods without observations and thus the PCE model fails to predict the future streamflow. To address this issue, the time-variant PCE coefficients are assumed to be related to the meteorological forcing variables (e.g., precipitation and temperature), and such a relationship can be characterized by deep neural networks (DNNs) and remain valid in the future. The input and output of DNNs are meteorological variables and PCE coefficients, respectively (see Figure 1 and the "Meteo" represents meteorological variables). Such an assumption enables efficient PCE-based hydrologic predictions by using well-calibrated DNNs to predict PCE coefficients for future periods without observations, even though the predicted PCE coefficients may not completely represent the behavior of hydrologic models.

To develop the DNN-based PCE for stochastic hydrologic predictions over the Dongjiang River Basin, we selected two widely used physically based hydrologic models, including the Variable Infiltration Capacity (VIC) model version 4 (Liang et al., 1994) and the Soil and Water Assessment Tool (SWAT) model (Arnold et al., 1998) (see Figure 1). Details on model setups are provided in Text S1 in Supporting Information S1. To develop the PCE-based surrogates for the two hydrologic models, the five most sensitive parameters were selected for each model based on sensitivity analyses (see the sensitivity analysis results in Figures S1 and S2 in Supporting Information S1 for the SWAT and VIC models, respectively) and previous studies (Ghaith & Li, 2020; Gou et al., 2020). Details on the parameter selection are provided in Text S2 in Supporting Information S1. Two five-dimensional second-order PCE-based surrogates were developed in this study for VIC and SWAT models, leading to two DNN-based PCE models, namely SWAT-PCE and VIC-PCE. The DNN-based PCE models were applied to predict daily discharges of the Longchuan and Boluo gauging stations, respectively (Figure 2c) for the

past and future periods. To estimate PCE coefficients for PCE-based hydrologic predictions, a 10-layer, the fully connected artificial neural network was constructed to relate PCE coefficients with areal mean daily maximum and minimum temperature, as well as 1-, 2-, 3-, 4-, 5-, 6-, 8-, 10-, 15-, 20-, 25-, 30-, 45-, 182 60-, 75-, and 90-day cumulative precipitation for the upstream contributing area since these variables are the dominant meteorological factors influencing catchment hydrologic characteristics (Ghaith & Li, 2020).

2.2. Vine Copula Multi-Model Ensemble Approach

As a single DNN-based PCE model is inadequate for reliable hydrologic predictions due to model structural uncertainty, the outputs from multiple DNN-based PCE models are expected to be combined to address the uncertainty in model structures for improving the reliability of hydrologic predictions. To this end, a vine copula multi-model ensemble approach is developed based on regular vine copulas to construct a joint PDF of streamflow time series generated from multiple hydrologic predictions and observations. The basic idea of this approach is to implement repeated conditional sampling from the well-calibrated vine copula given the predicted streamflow, thus generating multi-model ensemble predictions. Assume that $\boldsymbol{r} = (r_1,\ldots, r_{n-1}, r_n)$ signifies streamflow predictions generated from $n-1$ models and the corresponding observation. The joint PDF between predictions $(r_1,\ldots, r_{n-1})$ and the observation r_n can be expressed as

$$p(r_1, ..., r_{n-1}, r_n) = p_1(r_1) \cdot ... \cdot p_{n-1}(r_{n-1}) \cdot p_n(r_n) \cdot c(u_1, ..., u_{n-1}, u_n) \tag{7}$$

where $p_i(r_i)$ represents the marginal PDF and u_i represents the marginal cumulative probability, $i = 1,\ldots, n$; c represents the copula density. Since $c(u_1,\ldots, u_{n-1}, u_n)$ are inflexible in high dimensions and the high-dimensional copula families are limited, vine copula, also known as pair-copula construction (PCC), has been proposed to graphically represent Equation 7 as vines comprising a nested set of trees with nodes that are joined by edges (Bedford & Cooke, 2002). The canonical vine (C-vine) and the drawable vine (D-vine) are two special regular vines and are also the most widely used decompositions. Equation 7 can be decomposed through the C-vine and D-vine copulas as Equations 8 and 9, respectively.

$$p(r_1, ..., r_{n-1}, r_n) = \prod_{k=1}^{n} p_k(r_k) \prod_{j=1}^{n-1} \prod_{i=1}^{n-j} c_{j,j+i|1,\ldots,j-1} \{P(r_j|r_1, ..., r_{j-1}), P(r_{j+i}|r_1, ..., r_{j-1})\} \tag{8}$$

$$p(r_1, ..., r_{n-1}, r_n) = \prod_{k=1}^{n} p_k(r_k) \prod_{j=1}^{n-1} \prod_{i=1}^{n-j} c_{i,i+j|i+1,\ldots,i+j-1} \{P(r_i|r_{i+1}, ..., r_{i+j-1}), P(r_{i+j}|r_{i+1}, ..., r_{i+j-1})\} \tag{9}$$

where $P(\cdot|\cdot)$ represents the conditional cumulative probability. If hydrologic predictions from two models are combined, the joint density between the predictions (r_1, r_2) and the observation (r_o) can be decomposed through a 3-dimensional vine copula as

$$\begin{aligned} p(r_1, r_2, r_o) = {} & p(r_1) \cdot p(r_2) \cdot p(r_o) \cdot c(u_1, u_2, \alpha_{1,2}) \cdot c(u_1, u_o, \alpha_{1,o}) \cdot \\ & c(h(u_2, u_1, \alpha_{1,2}), h(u_o, u_1, \alpha_{1,o}), \alpha_{2,o|1}) \end{aligned} \tag{10}$$

where the h-function is the conditional distribution function (see details in Text S3 in Supporting Information S1); $\alpha_{1,2}$, $\alpha_{1,o}$, and $\alpha_{2,o|1}$ represent the parameters of bivariate copulas. There are multiple vine copula structures to decompose $p(r_1, r_2, r_o)$, the number of which grows exponentially with the number of variables. Thus, we use the sequential maximal spanning tree algorithm proposed by Diβmann et al. (2013) along with the Akaike information criterion (AIC) to identify an appropriate structure. When the vine structure is determined, a conditional cumulative distribution function (CDF) of r_o can be constructed by recursively applying the h-function:

$$P(r_o|r_1, r_2) = \frac{\partial C_{o,2|1}(P(r_o|r_1), P(r_2|r_1))}{\partial P(r_2|r_1)} = h\left[h(u_o, u_1, \alpha_{1,o}), h(u_2, u_1, \alpha_{1,2}), \alpha_{2,o|1}\right] \tag{11}$$

Thus, the inverse form of Equation 11 can be used to combine multi-model hydrologic predictions for generating probabilistic ensemble predictions:

$$\hat{r}_o = f(r_1, r_2, \tau) = P_o^{-1}\left\{h^{-1}\left(h^{-1}(\tau|h(P_2(r_2)|P_1(r_1), \alpha_{1,2}), \alpha_{2,o|1})|P_1(r_1), \alpha_{1,o}\right)\right\}, \tau \in (0, 1) \tag{12}$$

where τ represents random probability levels (e.g., τ = 0.01, 0.1,…, 0.99); P represents marginal CDFs. To achieve reliable model results, MC simulations are used to generate multiple (e.g., 500) samples of τ from the uniform distribution $U(0, 1)$, leading to multiple realizations of r_o. The median values of these realizations are obtained as hydrologic predictions, and the uncertainty intervals can be also derived.

To improve hydrologic predictions over the Dongjiang River Basin, the vine copula multi-model ensemble approach was used to combine model outputs from two DNN-based PCE models (see Section 2.1). In this approach, vine copula is used to construct a joint PDF of the streamflow generated from the observation and two PCE-based models for the past period, as shown in Equation 10. Since vine copula builds a multidimensional relationship between the two predictions and the observation in probability space, it is crucial to select appropriate univariate CDFs to convert the two predictions and the observation into uniform variables on the interval [0, 1]. Thus, a total of 9 probability distributions were examined, including gamma, log-normal, log-logistic, Gumbel, generalized extreme value (GEV), generalized Pareto (GP), log-gamma, generalized gamma, and four-parameter kappa (kappa4) distributions. The optimal marginal distribution was identified using the Kolmogorov-Smirnov (K-S) test, while the corresponding distribution parameters were estimated by the maximum likelihood method. Results indicate that the kappa4 distribution was selected for most cases except for the observation over the Boluo station at which the observation was fitted to the generalized gamma distribution (see results in Table S4 in Supporting Information S1). The Q-Q plots also indicate that the selected distributions are an appropriate choice (see Figure S3 in Supporting Information S1). The bivariate copula families considered in this study include Gaussian, Student t, Clayton, Gumbel, and Frank. To assess the robustness of the proposed approach, it is necessary to perform a quantitative comparison with previous approaches. BMA is one of the most widely used multi-model combination techniques in the hydroclimate community and is thus selected as the comparative benchmark (Raftery et al., 2005; B. Zhang & Wang, 2021). The selected BMA includes the normal and gamma BMA approaches that approximate the predictive PDFs by normal and gamma BMA distributions, respectively.

2.3. Vine Copula-Based Polynomial Chaos Framework

To integrate the DNN-based PCE with the vine copula multi-model ensemble approach, we propose a vine copula-based polynomial chaos framework to perform reliable and efficient multi-model hydrologic predictions, with the computational procedure described step by step as follows.

1. Select n sensitive parameters $\boldsymbol{\theta} = \{\theta_1, \theta_2,\ldots, \theta_n\}$ for each hydrologic model and determine their parameter ranges.
2. Determine sample points of $\boldsymbol{\xi} = \{\xi_1, \xi_2,\ldots, \xi_n\}$ using the regression-based collocation method and transform the sample points into the uniform space using the inverse of Equation 6.
3. Specify the sample points generated from step 2 as the parameter values of hydrologic models and obtain the corresponding time series of simulated streamflow $\boldsymbol{R}$ for each hydrologic model.
4. Estimate PCE coefficients $\hat{R}_j(t)$ for each time step t through the Hermite polynomials in Equation 3 based on the simulated streamflow $\boldsymbol{R}_t$.
5. Develop a multiple-layer (e.g., 10-layer), fully connected artificial neural network (ANN) to build relationships between PCE coefficients and climate variables (e.g., precipitation and temperature) for the past period. Then use the climate variables for the future period as inputs of the well-calibrated ANN to predict PCE coefficients for the future period.
6. Select the marginal distribution of PCE-simulated and observed streamflow for the past period. Then construct a conditional distribution of observed streamflow given the simulated streamflow through vine copula (see Section 2.2).
7. Generate n independent samples $\{\xi_1, \xi_2,\ldots, \xi_n\}$ of size m (e.g., 2,000) from the standard normal distribution. Then use PCE coefficients generated from step 5 and the n normal vectors $\{\xi_1, \xi_2,\ldots, \xi_n\}$ as inputs of Equation 5 to perform PCE-based hydrologic projections for the future period.
8. Transform the predicted streamflow for the future period generated from step 7 into uniform variables $\boldsymbol{u}$ using the selected marginal distribution in step 6. Then perform repeated sampling from the well-calibrated conditional vine copula in step 7 by specifying $\boldsymbol{u}$ as a conditioning variable, generating multi-model ensemble predictions for the future period.

2.4. Performance Metrics

To evaluate the PCE-based hydrologic prediction and the vine copula multi-model ensemble approach, five performance metrics are used, including reliability, sharpness, bias, efficiency, and a probabilistic scoring rule, continuously ranked probability score (CRPS). Reliability represents the consistency between the predictive distribution and observations and is assessed using the reliability metric of Evin et al. (2014), which quantifies the departure of the predictive quantile-quantile plot from the uniform distribution (Thyer et al., 2009). Sharpness, that is, the spread of the ensemble prediction members, is quantified as the ratio of the 90% limits of the predicted streamflow distribution and the 90% limits of the climatological streamflow distribution. Bias is the ratio of the mean streamflow generated from predictions and observations. CRPS is used to assess the overall performance since it addresses reliability and sharpness simultaneously, and the overall performance is expressed as a skill score (CRPSS) of the predictive distribution relative to the climatological streamflow distribution (Hersbach, 2000). The efficiency is indicated by the total time taken to complete 2,000 simulation runs. Note that the lower the reliability, sharpness, and efficiency metrics, the better the model prediction. The higher the CRPSS value, the better the model prediction. The closer to 1 the bias metric, the better the model prediction. More details of the performance metrics are provided in Text S5 in Supporting Information S1.

2.5. Uncertainty Decomposition

Since two DNN-based PCE models were used to project future changes in the streamflow regimes, an ANOVA-based variance decomposition method was used to partition the total ensemble uncertainty in the projected changes of streamflow regimes into two components including the PCE model parameter and structure. In this study, the total ensemble uncertainty is specified as the variance of the climate change signal in the mean annual cycle of streamflow and different streamflow quantiles. Although the SWAT and VIC models have different parameters, the parameters of PCE models developed in this study are the same, that is, five random variables sampled from the standard normal distribution. Since 2,000 simulations were performed through random parameter sampling using the SWAT- and VIC-based PCE models separately, there are a total of 4,000 (2,000 parameter sets × 2 model structures) model combinations. Thus, a two-factor (parameter and structure) ANOVA model was constructed to split the total sum of the squares (SST) into sums of squares (SS) due to the individual effects and their interaction as

$$\mathrm{SST} = \mathrm{SS_s} + \mathrm{SS_p} + \mathrm{SS_{sp}} \tag{13}$$

where $\mathrm{SS_s}$ and $\mathrm{SS_p}$ represent the SS due to the effects of structures and parameters of the PCE models, respectively; $\mathrm{SS_{sp}}$ represents the SS due to the combined effects of structures and parameters of the PCE models. It should be noted that the interaction among five parameters of PCE models is not quantified in this study because the parameters are assumed to be independent. Such a method can provide estimates of the fraction of the total uncertainty attributable to each source, expressed as the variance fraction η^2. Values of 0 and 1 for η^2 represent a contribution of 0% and 100% to the total ensemble uncertainty, respectively. Details of the ANOVA-based variance decomposition method are provided in Text S6 in Supporting Information S1.

2.6. Multi-Decadal Convection-Permitting Climate Modeling

To generate high-resolution climate information for projecting future changes in hydrologic regimes, the WRF model was used to perform multi-decadal convection-permitting climate projections over the GBA. The model configuration follows a two-way triple nesting setup with the outer two domains consisting of simulations with parameterized convection (D01 and D02), and the innermost domain of a simulation with the parameterization of deep convection switched off (D03), as shown in Figure 2a. The outermost domain D01 covers a large part of China with 68 × 56 grid points at a 36 km resolution, while the nested domain D02 is resolved at a 12-km grid spacing (138 × 96 grid points). The innermost domain D03 covers the GBA at a 4-km grid spacing (216 × 171 grid points). The vertical direction is discretized using 21 stretched model levels topped at 50 hPa. Details of the parameterization schemes used in the WRF simulations are provided in Text S4 in Supporting Information S1.

Convection-permitting simulations were separately conducted for the historical (1980–2005) and future (2074–2099) periods to assess climate change impacts on regional hydroclimatic regimes. The historical simulation was forced by the European Center for Medium Range Weather Forecasting (ECMWF) reanalysis product,

ERA-Interim, which has a 6-hr temporal resolution and a 0.75° × 0.75° spatial resolution (Dee et al., 2011). The future projection was forced with the ERA-Interim reanalysis consecutively perturbed using the Pseudo-Global Warming (PGW) technique and global climate model (GCM) ensembles (Y. Li et al., 2019; S. Wang & Wang, 2019). In the PGW method, the future force was given by the combination of reanalysis data and a perturbated estimation from a 30-year ensemble of 10 GCMs from the Coupled Model Intercomparison Project Phase 5 (CMIP5) under the Representative Concentration Pathway 8.5 (RCP8.5) (Equation 14) since a 30-year period is needed to examine extremes within a climate system (Jing et al., 2019).

$$\mathrm{PGW}_{\mathrm{forcing}} = \mathrm{ERA} - \mathrm{Interim} + (\mathrm{CMIP5}_{2071-2100} - \mathrm{CMIP5}_{1976-2005}) \quad (14)$$

The perturbed physical fields include temperature, geopotential, specific humidity, horizontal wind, sea surface temperature, sea level pressure, and soil temperature. The use of the PGW technique overcomes the substantial inter-model variability among GCMs and greatly reduces the computational cost by avoiding a continuous simulation spanning a century (Y. Li et al., 2019). The 10 GCMs were selected based on their performance in reproducing the historical climate over China (Chen & Frauenfeld, 2014; Jiang et al., 2015), and their details are provided in Table S1 in Supporting Information S1.

2.7. Data Sources

The MSWEP V2 (Multi-source weighted-Ensemble Precipitation, version 2) 0.1° daily-precipitation product was used to evaluate the WRF-simulated precipitation in South China over the historical period, while the ERA5-Land 0.1° reanalysis product was used to evaluate the simulations of daily maximum and minimum temperatures (Beck et al., 2019; Hersbach et al., 2020). The meteorological forcing data of the SWAT and VIC hydrologic models were collected from the MSWEP and ERA5-Land products as well as the in-situ observations (Figure 2c). Details of the meteorological forcing data can be seen in Text S1 in Supporting Information S1. To allow intuitive use and open access to the high-resolution climate information, a web-based data portal, known as China's Greater Bay Area Climate Data Portal (GBAcdp), was also established to visualize the convection-permitting WRF model outputs in terms of long-term trends, averages, and extremes (http://www.gbacdp.cn/). More details of the GBAcdp can be found in Qing and Wang (2021).

The Dongjiang River Basin is located in the east of the Pearl River Basin, South China (Figure 2b) with annual mean streamflow of 25.7 billion cubic meters and is a major water supply source for the GBA. To perform hydrologic predictions over the Dongjiang River Basin, a total of 25 years of daily streamflow from January 1981 to December 2005 was collected for the Longchuan and Boluo gauging stations, which have drainage areas of 7,699 km^2 and 25,325 km^2, respectively. The year 1980 was omitted since the EAR5-Land product was available only from 1981 onwards. And the first year (1981) was used as a spin-up period to reduce the sensitivity to the state-value initialization. The streamflow gauged at the Boluo station was potentially influenced by three major reservoirs, namely the Fengshuba, Xinfengjiang, and Baipenzhu in the upper, middle, and lower reaches of the river, which went into operation in 1974, 1962, and 1985, respectively. The streamflow gauged at the Longchuan station was potentially influenced by only the Fengshuba reservoir. To consider reservoir operations in hydrologic predictions, rule curves are a widely used approach to represent the storage dynamics of water reservoirs. We used the rule curves conceived to minimize the peak flow in the SWAT and VIC hydrologic models since the information on reservoir operating objectives is unavailable. The measured daily outflow time series were also collected for the three reservoirs from January 1981 to December 2005 to better represent reservoir operations.

3. Results

3.1. Construction of DNN-Based PCE Models for Efficient Stochastic Hydrological Prediction

The DNN-based PCE models were developed for improving the efficiency of hydrologic simulations over the Dongjiang River Basin during 1982–2005. The PCE-simulated daily streamflow is consistent with those generated from physically based hydrologic models (SWAT and VIC) (see Figures S4 and S5 in Supporting Information S1). The correlation coefficients are greater than 0.99 and 0.9 in terms of mean values and standard deviations, respectively. Such a consistency verifies that the PCE models can adequately capture the behavior of physically based hydrologic models during the period of 1982–2005, but the constructed PCE models fail to predict streamflow beyond the period since the time-variant PCE coefficients are only available during

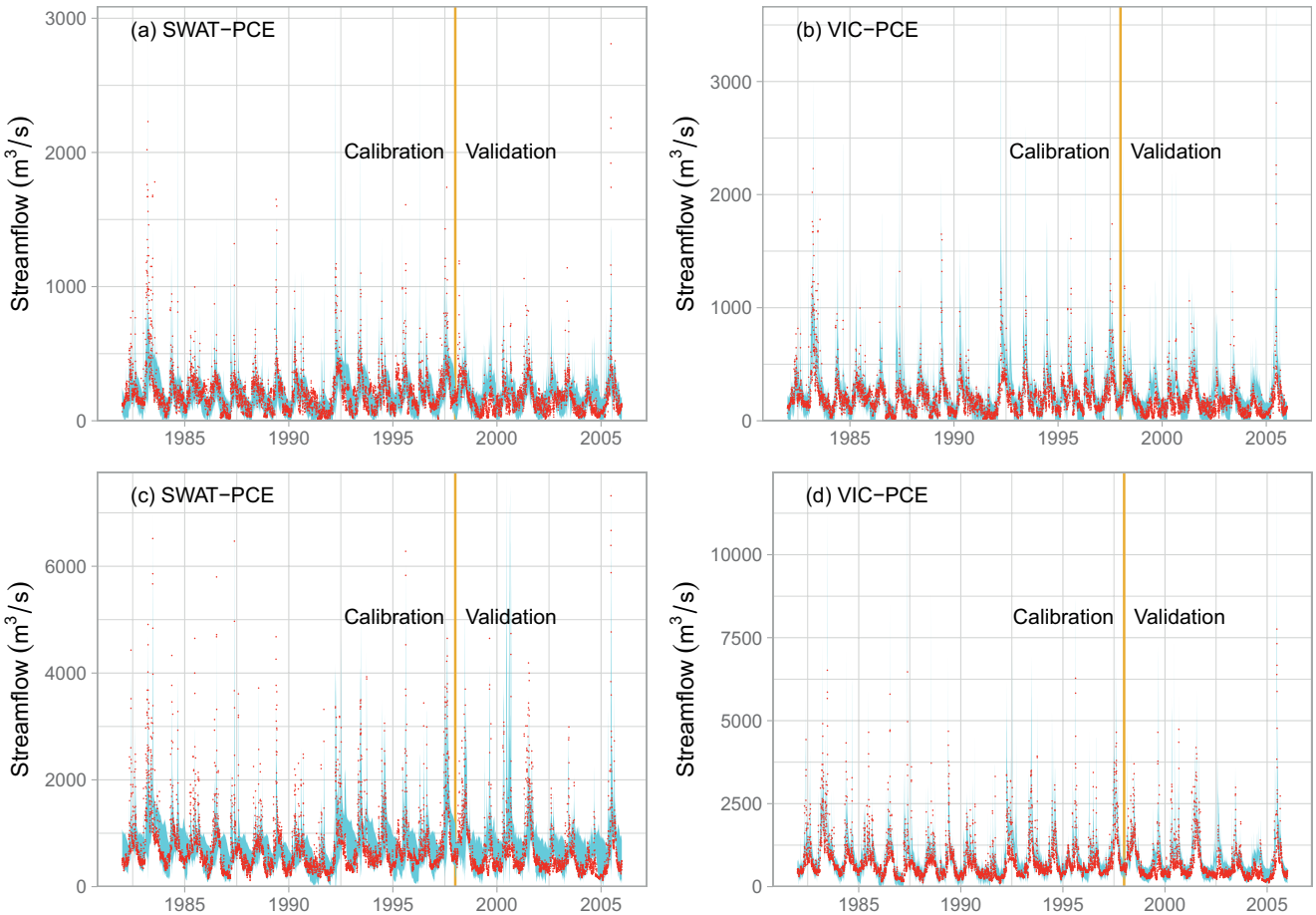

Figure 3. Daily streamflow predictions generated through SWAT- and VIC-based PCE models (namely SWAT-PCE and VIC-PCE) for the (a, b) Longchuan and (c, d) Boluo hydrologic stations over the calibration period of 16 years (1982–1997) and the validation period of 8 years (1998–2005). The light blue area represents the predicted streamflow time series with 95% uncertainty intervals. Red dots represent streamflow observations. SWAT = Soil and Water Assessment Tool; VIC = Variable Infiltration Capacity; PCE = polynomial chaos expansion.

1982–2005. To enable PCE-based hydrologic predictions for future periods without hydrologic observations, it is assumed that the multidimensional relationship between PCE coefficients and climate variables can be well characterized by DNNs and remains time-invariant. To verify the assumption, the DNNs were calibrated during 1982–1997 and then validated during 1998–2005 by predicting PCE coefficients and comparing the corresponding PCE-based predictions against streamflow observations. Figure 3 presents daily streamflow predictions with the 95% uncertainty ranges, generated from the SWAT-PCE and VIC-PCE models in the calibration period 1982–1997 and the validation period 1998–2005 for the Longchuan and Boluo gauging stations. In general, the predicted streamflow time series match well with the observation for the calibration and validation periods, albeit some high flows are not well captured. Specifically, more than 80% of observations fall within the 95% uncertainty range of streamflow predictions generated by the PCE models over both stations for the calibration period 1982–1997; the corresponding proportion is generally over 70% for the validation period 1998–2005. This indicates that the constructed DNN-based PCE models can well predict streamflow regimes over the Dongjiang River Basin.

To verify the superiority of the DNN-based PCE models, a total of 2,000 PCE-based simulations were performed to compare with 2,000 MC simulations using the SWAT and VIC models. Figure 4 presents a comparison of hydrologic predictions generated from the 2,000 PCE and MC runs in terms of reliability, sharpness, bias, CRPSS, and efficiency. In general, the PCE-based simulations and the MC-based hydrologic model simulations lead to a comparable performance in terms of reliability, sharpness, and bias, particularly for the validation period which is our main focus in hydrologic predictions. For example, the MC and PCE simulations achieve median reliability

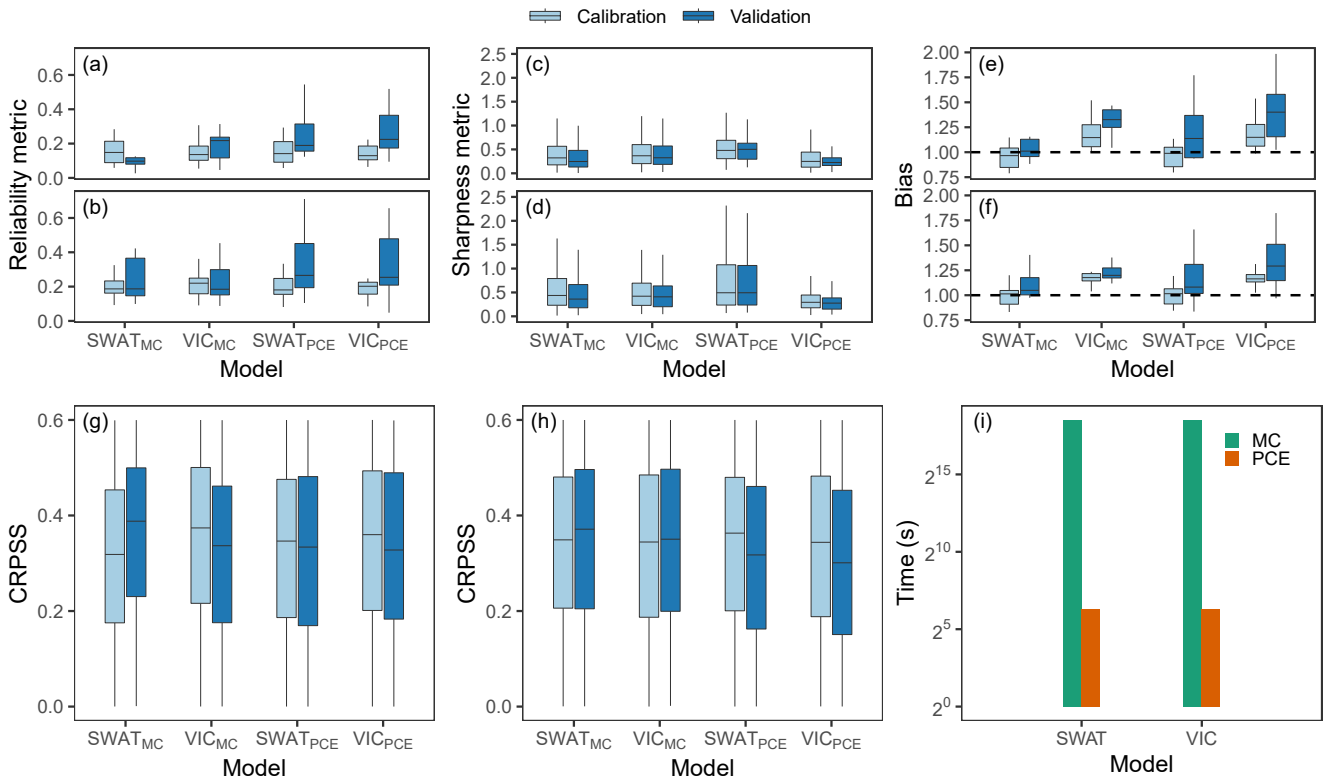

Figure 4. Comparison between hydrologic models ($SWAT_{MC}$ and VIC_{MC}) and DNN-based PCE models ($SWAT_{PCE}$ and VIC_{PCE}) in terms of (a, b) reliability, (c, d) sharpness, (e, f) bias, and (g, h) CRPSS, and (i) efficiency across years during the calibration (1982–1997) and validation (1998–2005) periods. (a, c, e, g) and (b, d, f, h) correspond to the Longchuan and Boluo gauging stations, respectively. MC = Monte Carlo; CRPSS = continuous ranked probability skill score. The thick black horizontal bars in (a–h) represent the median value, and the lower and upper edges of the box represent the 25th (Q_1) and 75th (Q_3) percentile values, respectively. The upper and lower edges of vertical lines represent the values of $Q_3 + 1.5 \times IQR$ and $Q_1 - 1.5 \times IQR$, respectively, where IQR denotes the interquartile range that is equal to $Q_3 - Q_1$.

of 0.22 based on the VIC model over the validation period 1998–2005 for the Longchuan gauging station (see Figure 4a). Such predictive capacities indicated by the PCE-based simulations, however, require substantially less computational time than the MC-based hydrologic model simulations (see Figure 4i). Specifically, it took (a desktop with an Intel® Core™ Processor i7-8700 CPU and 16 GB installed RAM) more than 4 days to complete 2,000 MC runs for a period of 24 years based on the SWAT and VIC models, but it took less than 80 seconds to complete 2,000 PCE runs for the same period. With similar predictive performance, the DNN-based PCE models are more than 4,000 times faster than the physically based hydrologic models. It should be noted that such an increase in the computational speed would vary with different setups of hydrologic models and the application of parallel computing frameworks.

To evaluate the robustness of stochastic hydrologic predictions based on the DNN-based PCE models, 10-fold cross-validation was also performed to compare the predicted streamflow time series generated from the PCE- and MC-based simulations. Figure 5 shows the scatter plots of the 10-fold cross-validation results in terms of mean and standard deviation. Results indicate that mean values and standard deviations of daily streamflow obtained from the PCE-based predictions agree well with those from the physically based hydrologic models (SWAT and VIC), which further verifies the capability of the DNN-based PCE models in predicting streamflow regimes and quantifying the underlying uncertainty. For example, the Pearson's *r* between the SWAT-PCE prediction and the SWAT-based hydrologic prediction is 0.94 and 0.87 in terms of mean values and standard deviations, respectively, over the Longchuan station (see Figures 5b and 5f). Therefore, the DNN-based PCE models can achieve computationally efficient probabilistic predictions of streamflow regimes with similar predictive capacities to physically based models.

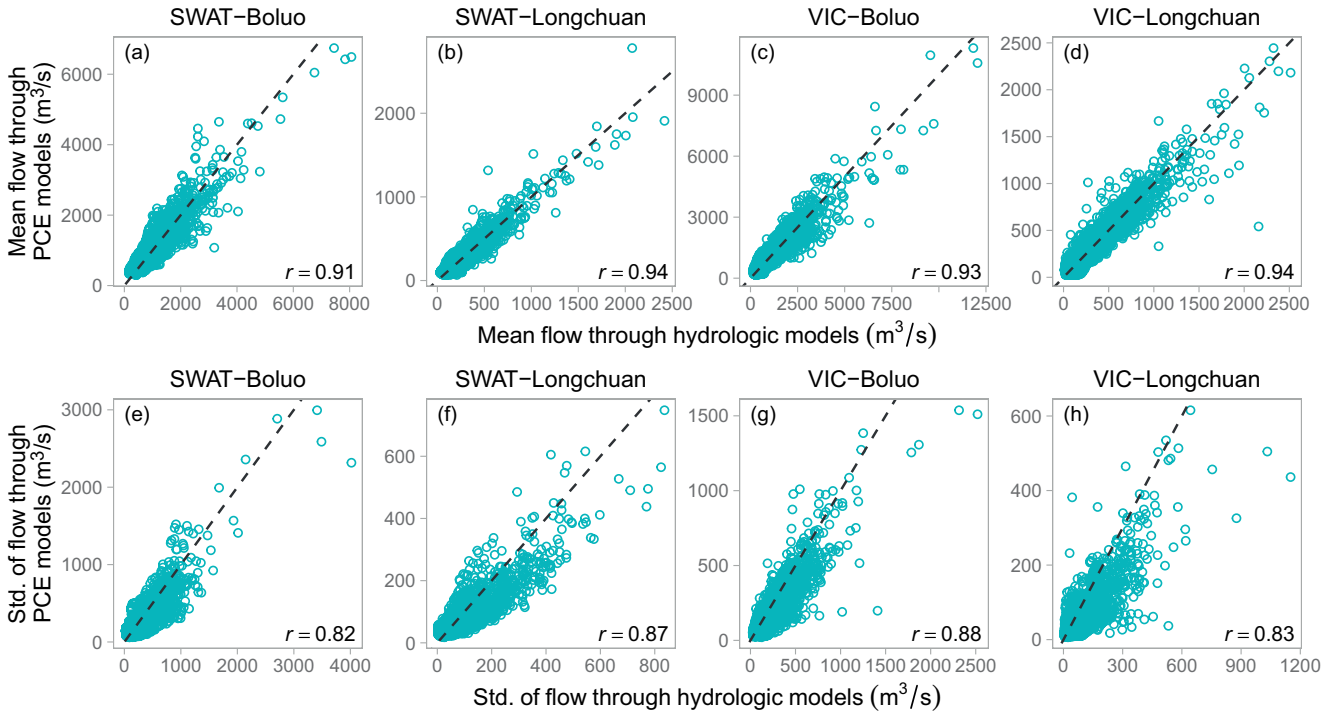

Figure 5. Scatter plots of the 10-fold cross validation for probabilistic streamflow predictions generated through hydrologic models (SWAT and VIC) and DNN-based PCE models constructed based on the SWAT and VIC models in terms of (a–d) the mean values and (e–h) the standard deviation (Std.) over the Longchuan and Boluo stations.

3.2. Multi-Model Ensemble Stochastic Hydrological Prediction

Since each of the physically based models (SWAT and VIC) has its advantages and limitations, no single model (SWAT-PCE or VIC-PCE) can outperform others in every aspect. The vine copula multi-model ensemble approach was used to combine stochastic hydrologic predictions generated from two DNN-based PCE models, leading to a multi-model ensemble prediction. Figure 6 presents the daily streamflow predictions with the 95% uncertainty range generated from the ensemble predictions for the Longchuan and Boluo stations over the calibration (1982–1997) and validation (1998–2005) periods. Results show that the predicted streamflow time series match well with observations, with the Pearson correlation coefficients, which represent the linear relationship between observations and mean values of predicted streamflow, greater than 0.8 for both stations over the validation period. The multi-model ensemble predictions also capture more observations within the confidence intervals

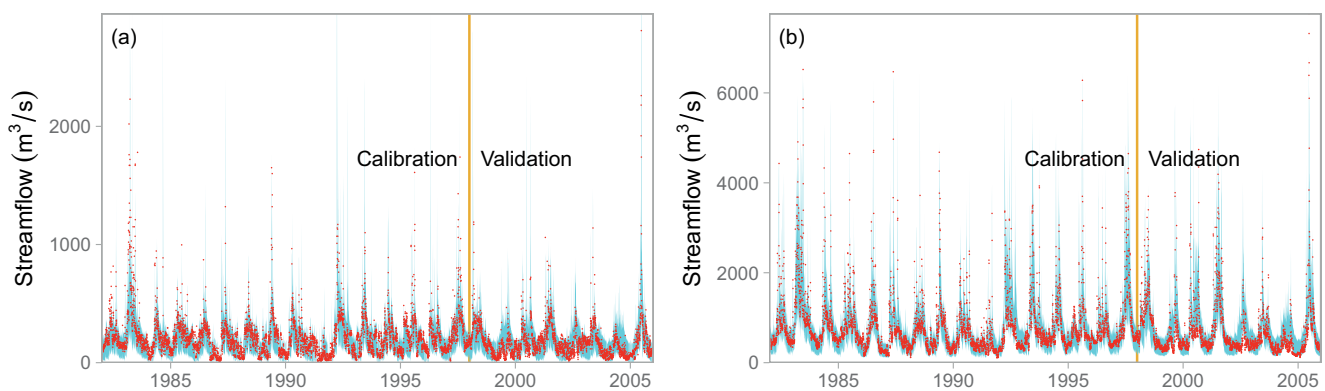

Figure 6. Probabilistic streamflow predictions generated by combining the SWAT-PCE and VIC-PCE models using the vine copula multi-model ensemble approach for the (a) Longchuan and (b) Boluo hydrologic stations over the calibration period of 16 years (1982–1997) and the validation period of 8 years (1998–2005). The light blue area represents the predicted streamflow time series with 95% uncertainty intervals. Red dots represent streamflow observations.

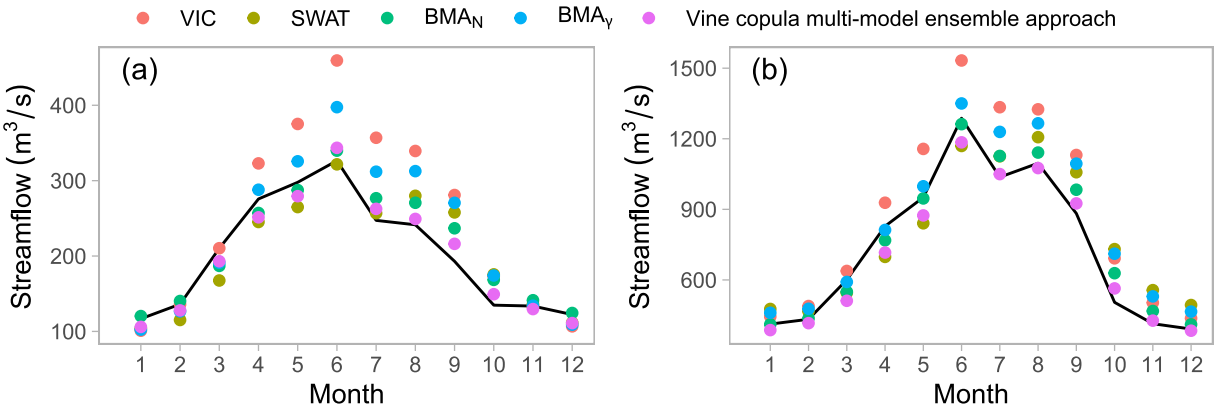

Figure 7. Comparison of the annual cycle of streamflow generated by individual SWAT-PCE and VIC-PCE models, as well as the multi-model ensemble simulation using BMA techniques and the vine copula multi-model ensemble approach for the (a) Longchuan and (b) Boluo hydrologic stations. The black line represents annual cycles of the observed streamflow. BMA_N and BMA_γ represent that the predictive PDF in BMA is approximated by normal and gamma distributions, respectively. BMA = Bayesian model averaging.

than the single DNN-based PCE predictions, indicating higher reliability of ensemble streamflow predictions. Specifically, the percentages of captured observations at the Longchuan station show a significant improvement from 78% (SWAT-PCE) and 77% (VIC-PCE) to 91% for the ensemble predictions over the validation period, while the percentages for the Boluo station also show a substantial improvement from 72% (SWAT-PCE) and 73% (VIC-PCE) to 89% for the ensemble predictions over the validation period. Thus, the vine copula-based multi-model ensemble prediction substantially enhances the reliability of hydrologic predictions in comparison with those generated by the single DNN-based PCE models.

To compare the vine copula multi-model ensemble approach with the BMA technique, Figure 7 presents the annual cycles of observed (black lines) and predicted streamflow for the Longchuan and Boluo stations during 1982–2005. Results show that the annual cycles of predicted streamflow well match with those of observations for both stations, and the vine copula multi-model ensemble approach generally improves the consistency between observed and predicted streamflow regimes compared to the single DNN-based PCE models. For example, the VIC-PCE model generally overpredicts streamflow in the warm season (April−September), whereas the SWAT-PCE model underpredicts spring (March−May) streamflow and overpredicts summertime (June−August) streamflow. Such biases can be greatly reduced by the vine copula multi-model ensemble approach. Specifically, the summertime streamflow generated by the SWAT-PCE and VIC-PCE models has positive biases of 350 and 580 m^3/s, respectively, over the Boluo station, which are reduced to 283 m^3/s by using the vine copula multi-model ensemble approach. Furthermore, the vine copula multi-model ensemble approach leads to smaller biases than the BMA in most cases, especially for the prediction of streamflow regimes from July to September. Specifically, the streamflow generated by the normal BMA (BMA_N), the gamma BMA (BMA_γ), and the vine copula multi-model ensemble approach have positive biases of 267, 379, and 197 m^3/s, respectively, over the Boluo station from July to September.

To further compare the vine copula multi-model ensemble approach with the BMA approaches in terms of ensemble hydrologic predictions, Figure 8 presents a comparison of hydrologic predictions generated by different evaluation metrics in terms of reliability, sharpness, bias, and CRPSS over the validation period 1998–2005. As lower values are better for the reliability metric, the BMA predictions are more reliable than the single DNN-based PCE predictions for the Boluo station but are less reliable for the Longchuan station (Figure 8a). In comparison, the vine copula multi-model ensemble approach leads to more reliable predictions than other approaches for both stations. Figures 8b–8c also show that hydrologic predictions generated from the vine copula multi-model ensemble approach are generally sharper and less biased than those generated from other techniques. In terms of the combined performance (CRPSS), the vine copula multi-model ensemble approach and the SWAT-PCE model obtain similar results for the Longchuan station, but the former leads to the highest CRPSS value for the Boluo station. In comparison, the BMA approaches lead to lower CRPSS values than the SWAT-PCE model for the Longchuan station. This indicates that the vine copula multi-model ensemble approach outperforms the BMA techniques in combining multiple model outputs in terms of reliability, sharpness, and accuracy. Such an

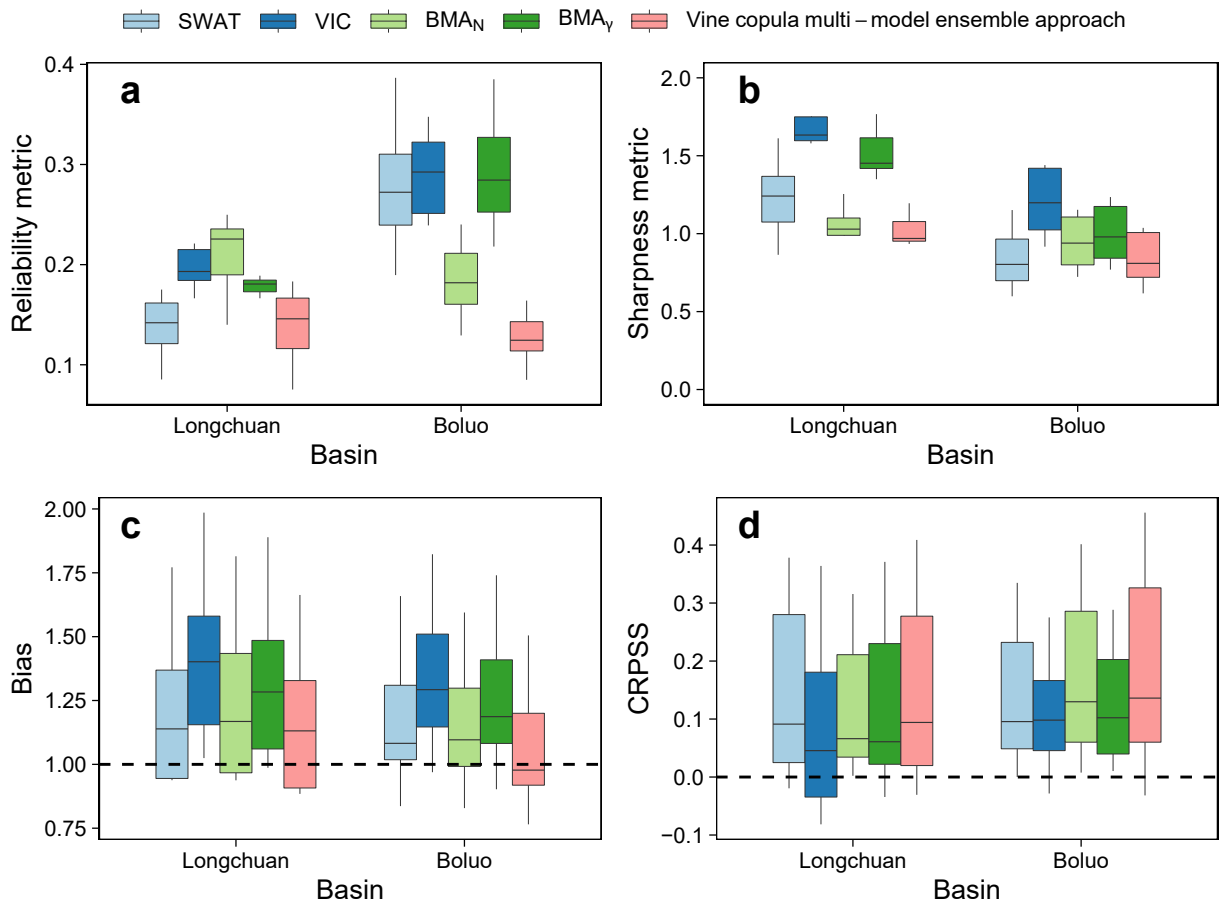

Figure 8. Comparison of model performance in hydrologic predictions indicated by (a) reliability, (b) sharpness, (c) bias, and (d) CRPSS across years over the validation period 1998–2005. $SWAT_{PCE}$ and VIC_{PCE} represent the SWAT-PCE and VIC-PCE models, respectively. The boxplots are created with the same setting as Figure 4.

improvement results from the flexible structure of the vine copula-based approach, which relaxes the assumption of the shapes of posterior distributions in the BMA approach.

3.3. Probabilistic Hydroclimatic Projection at a Convection-Permitting Scale

To project future hydrologic response to the changing climate at a river basin scale, the convection-permitting WRF climate simulation was performed in this study to generate the relevant climate variables including daily precipitation, and daily maximum and minimum temperature. Figure 9 presents the spatial patterns of absolute and relative model biases of annual precipitation and minimum and maximum temperatures. The WRF-simulated annual precipitation has a wet bias over the northern part of the Dongjiang River Basin and has a dry bias over the southern part against the MSWEP precipitation. The relative biases are generally less than 50% over the Dongjiang River Basin (Figure 9d). The WRF-simulated minimum temperature shows a model bias of less than 1°C and a relative bias of less than 15%. In comparison, the WRF model tends to overestimate the maximum temperature over most of the simulation domain, and the corresponding relative bias is generally less than 10%. Thus, the WRF model is skillful in simulating temperature and precipitation over the study domain, ensuring the reliability of regional hydroclimatic projections.

Figure 10 depicts the comparison of the 24-year annual precipitation, and minimum and maximum temperatures under past and future climates. The future annual precipitation amount over the Dongjiang River Basin ranges from 1,000 to 2,500 mm. The absolute difference is less than 200 mm and the relative difference is less than 30% for the entire domain. On the other hand, the WRF model projects an overall increase in annual minimum and

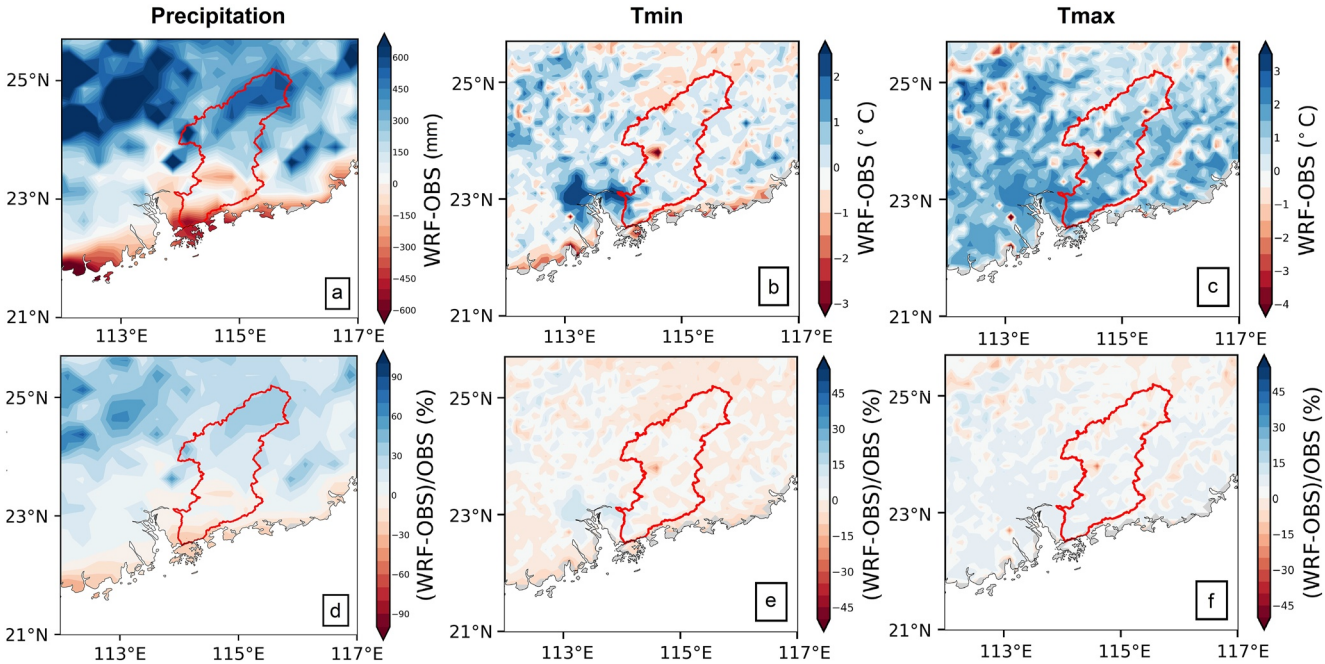

Figure 9. Spatial patterns of (a–c) absolute model bias and (d–f) relative model bias for annual precipitation, minimum (T_{min}) and maximum (T_{max}) temperatures during 1982–2005.

maximum temperatures over the entire domain under RCP8.5. For example, the absolute increment in maximum temperature ranges from 2.4°C to 4.8°C. It can be also seen that the relative increment in maximum temperature is generally less than that in minimum temperature. Such differences induced by global warming have the potential to alter regional hydrologic regimes over the Dongjiang River Basin.

Extreme precipitation plays a crucial role in changing regional hydrologic regimes and in triggering water-related hazards, such as floods and droughts. Figure 11 exhibits the absolute and relative differences of the 24-year mean precipitation extremes between past and future climates. Four extreme precipitation indices were used in this study, including very wet days (R95pTOT), extremely wet days (R99pTOT), and maximum 1-day and 5-day precipitation (Rx1day and Rx5day). The definition of these indices is provided in Table S5 in Supporting Information S1. The R95pTOT, R99pTOT, and Rx5day are projected to increase for most of the Dongjiang River Basin, especially for the northern part, by up to 80%, 120%, and 60%, respectively. In comparison, the Rx1day does not show a significant increase, especially in the east of the Dongjiang River Basin. The southeastern part of the Dongjiang River Basin is also projected to have a slight decrease in the Rx1day and Rx5day.

The projected future precipitation and temperature were used to force the DNN-based SWAT-PCE and VIC-PCE models, generating future changes in probabilistic streamflow time series (see Figure S6 in Supporting Information S1). To improve the reliability of streamflow projections, the two probabilistic streamflow time series, generated by DNN-based SWAT-PCE and VIC-PCE models, were combined by the vine copula multi-model ensemble approach. Figure 12 presents the projected future changes in areal mean precipitation for the upstream contributing areas of the Longchuan and Boluo stations over a 24-year period (2076–2099), as well as the predicted daily streamflow time series with the 95% uncertainty range. The upstream contributing areas of the Longchuan and Boluo stations are projected to experience a substantial increase (as large as 54% and 59%) in the number of R99p heavy rainfall events for the future period 2076–2099 compared to the historical period 1982–2005. The total precipitation of R99pTOT is projected to increase by 51% and 56% over the Longchuan and Boluo stations, respectively, for the future period 2076–2099. Such increases in extreme precipitation lead to increases in the number and magnitude of high-flow events in the future period 2076–2099. Specifically, the Longchuan and Boluo stations are projected to experience 76 [58–95] and 39 [16–54] peak flow events, respectively, with daily streamflow exceeding the historical 99th percentile for the future period 2076–2099. The number of future peak

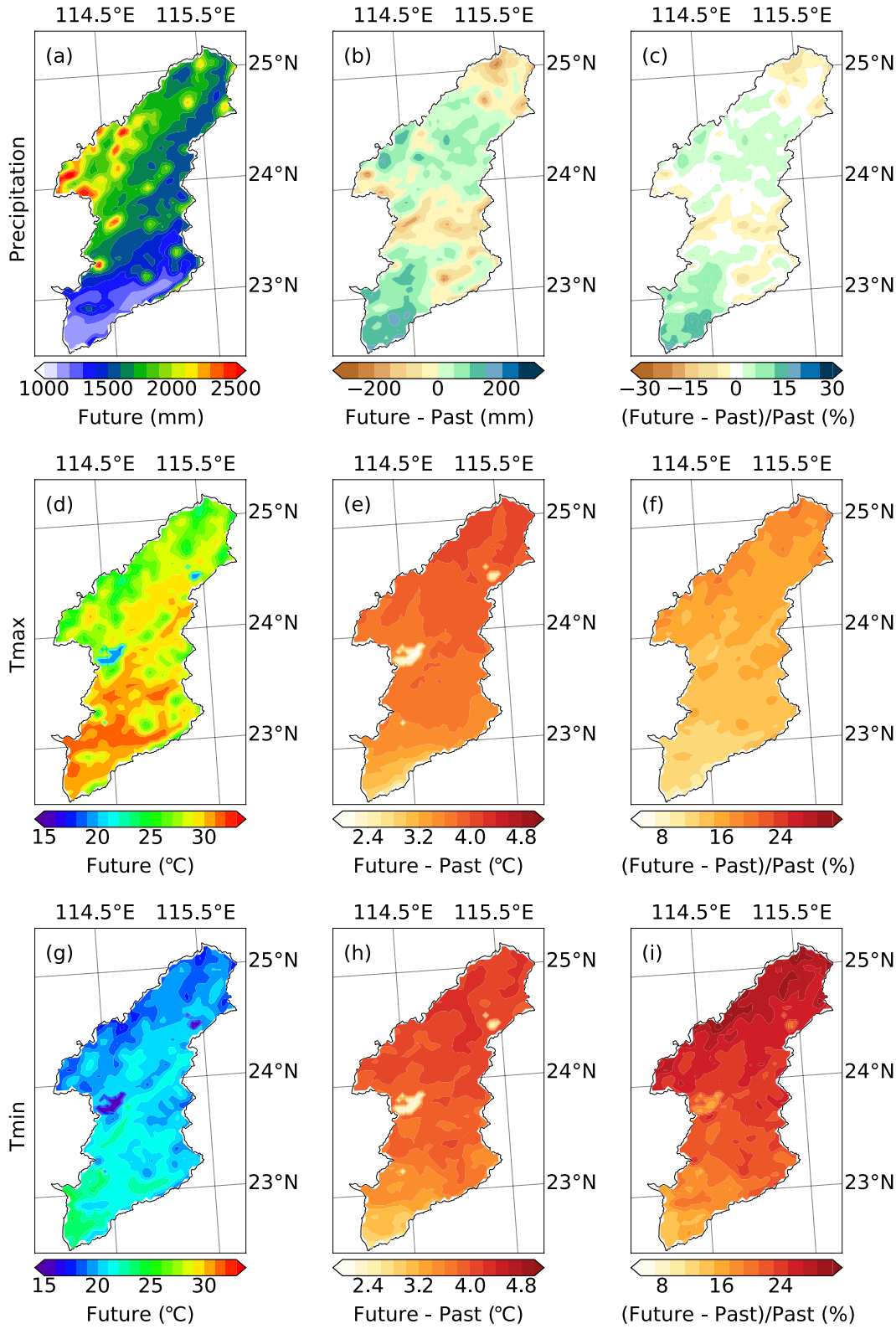

Figure 10. Spatial patterns of 24-year annual precipitation, minimum (T_{min}) and maximum (T_{max}) temperatures for (a, d, g) the future climate, (b, e, h) the absolute and (c, f, i) the relative differences between past and future climates.

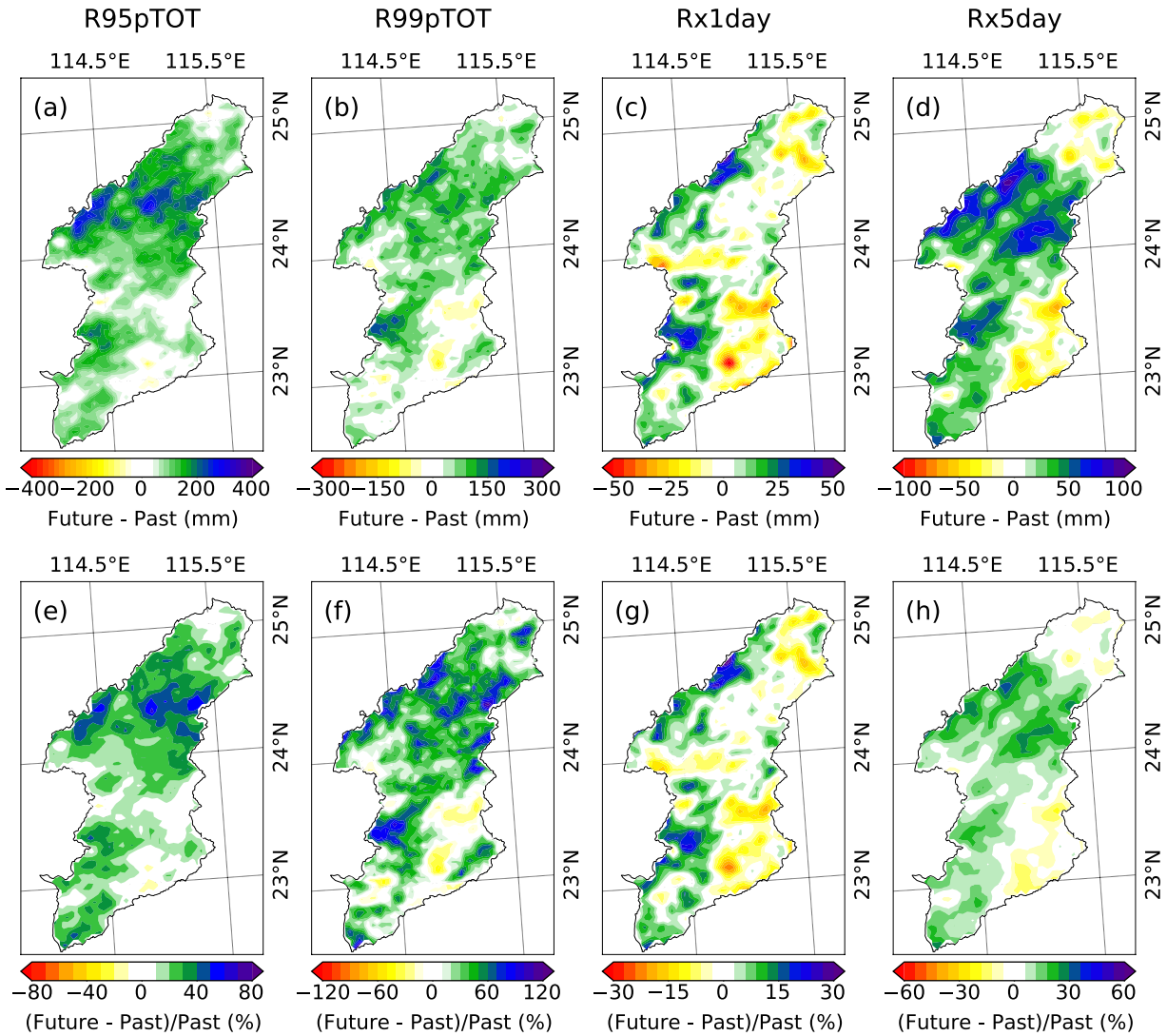

Figure 11. (a–d) Absolute and (e–h) relative differences of 24-year mean precipitation extreme (R95pTOT, R99pTOT, Rx1day, Rx5day) between past and future climates.

flow events projected for the Longchuan and Boluo stations is larger than the 37 and 31 events, respectively, detected in the historical period 1982–2005.

To further assess regional hydrologic regimes in response to climate change, Figure 13 presents annual streamflow cycles, the mean and extreme streamflow, as well as the flood magnitudes estimated under historical and future climates. Figure 13a shows that the high-flow season timing at the Longchuan station is projected to remain unchanged with a 13% [11%–15%] increase in the summer streamflow (June–August) for the future period 2076–2099 compared to the historical period 1982–2005. In comparison, the high-flow season at the Boluo station is projected to begin earlier in late spring (May) with a decrease of 12% [11%–13%] in the summer streamflow but an increase of 7% [6%–9%] in the spring streamflow (March–May). Although the mean streamflow is projected to witness little change (Figure 13c), the annual mean maximum streamflow will significantly increase by 25% [8%–69%] over the Longchuan station (Figure 13d). Such increases, however, are not significant for the Boluo station with changes falling within the range −28%–10%. Such different changes in the projected annual maximum streamflow lead to the difference in flood risk assessments (see Figures 13e and 13f). The flood magnitudes are estimated by first defining the Peaks over Threshold (POT) samples using the tenth percentile of the annual maximum streamflow as a threshold and then fitting the generalized Pareto distribution (GP) (see

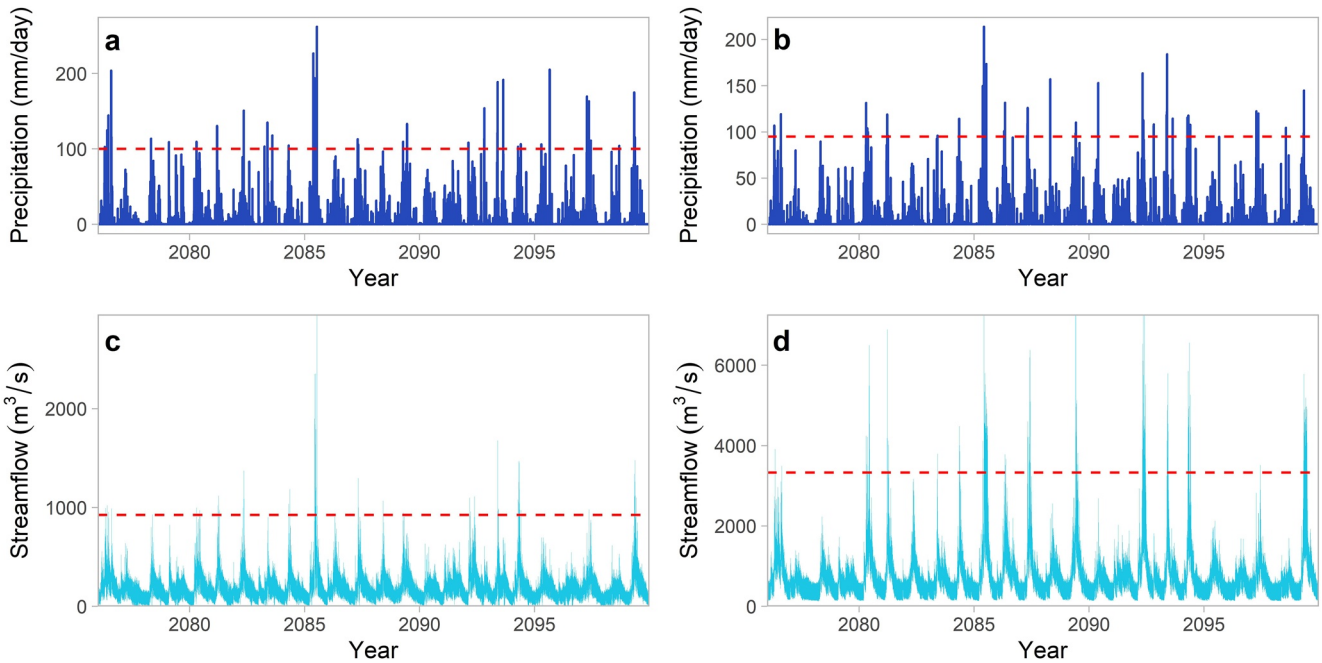

Figure 12. Multi-model ensemble projections of daily streamflow generated through combining the SWAT-PCE and VIC-PCE models using the vine copula multi-model ensemble approach for the (c) Longchuan and (d) Boluo hydrologic stations by the end of the twenty-first century. The light blue area represents the projected streamflow time series with 95% uncertainty intervals. (a) and (b) correspond to projected precipitation for the upstream contributing area of the Longchuan and Boluo hydrologic stations, respectively. The red dashed lines in (a–b) and (c–d) represent the 99th percentiles of historical precipitation and streamflow, respectively.

details in Brunner et al., 2020). In general, the Longchuan station is projected to experience substantial increases in the flood magnitudes for the future period 2076–2099 compared to the historical period 1982–2005, but such increases are not significant for the Boluo station. For example, the estimated magnitude of the 20-year flood is 2,413 m^3/s [1,574–3,252 m^3/s] over the Longchuan station for the historical period 1982–2005, but the estimated 20-year flood magnitude is projected to increase to 3,337 m^3/s [1,475–6,081 m^3/s] for the future period 2076–2099. In comparison, the projected changes in the estimated magnitude of the 20-year flood over the Boluo station range from −67% to 113% with a mean value of 9%. The difference in the projected increases of flood magnitudes can be related to the reservoir operation represented in stochastic simulations, which is based on the rule curves conceived to minimize the peak flow (Duc Dang et al., 2020). Such a reservoir operation rule may potentially offset the impacts of increased extreme precipitation on peak flows, thereby leading to little change in the projected flood magnitudes over the Boluo station that is affected by three reservoirs (Brunner, 2021). It should be also noted that the future hydrologic regimes are projected under RCP8.5 and would vary under different emissions pathways and different reservoir rule curves used.

4. Discussion

In this study, we have developed two DNN-based PCE models (SWAT-PCE and VIC-PCE) to perform probabilistic projections of future hydrologic regimes under a changing climate. The integration of DNNs and PCE models enables the quantification of the dependence between the response models of catchment processes and climate regimes. This raises the question of how the DNN-based PCE model structures and parameters contribute to the overall uncertainty in hydrologic projections. To address this question, the ANOVA-based variance decomposition method was used to partition the total ensemble uncertainty in the projected changes of streamflow regimes into two components including the PCE model parameter and structure (Bosshard et al., 2013). Figure 14 presents the annual cycle of historical streamflow and the variance decomposition of climate change signals in the mean annual cycle of streamflow. Results show that the model structural uncertainty makes a substantial contribution to the total uncertainty with mean values of 63% and 46% for the Longchuan and Boluo stations, respectively. Model structures become the dominant source of uncertainty at the Longchuan station in the high-flow season

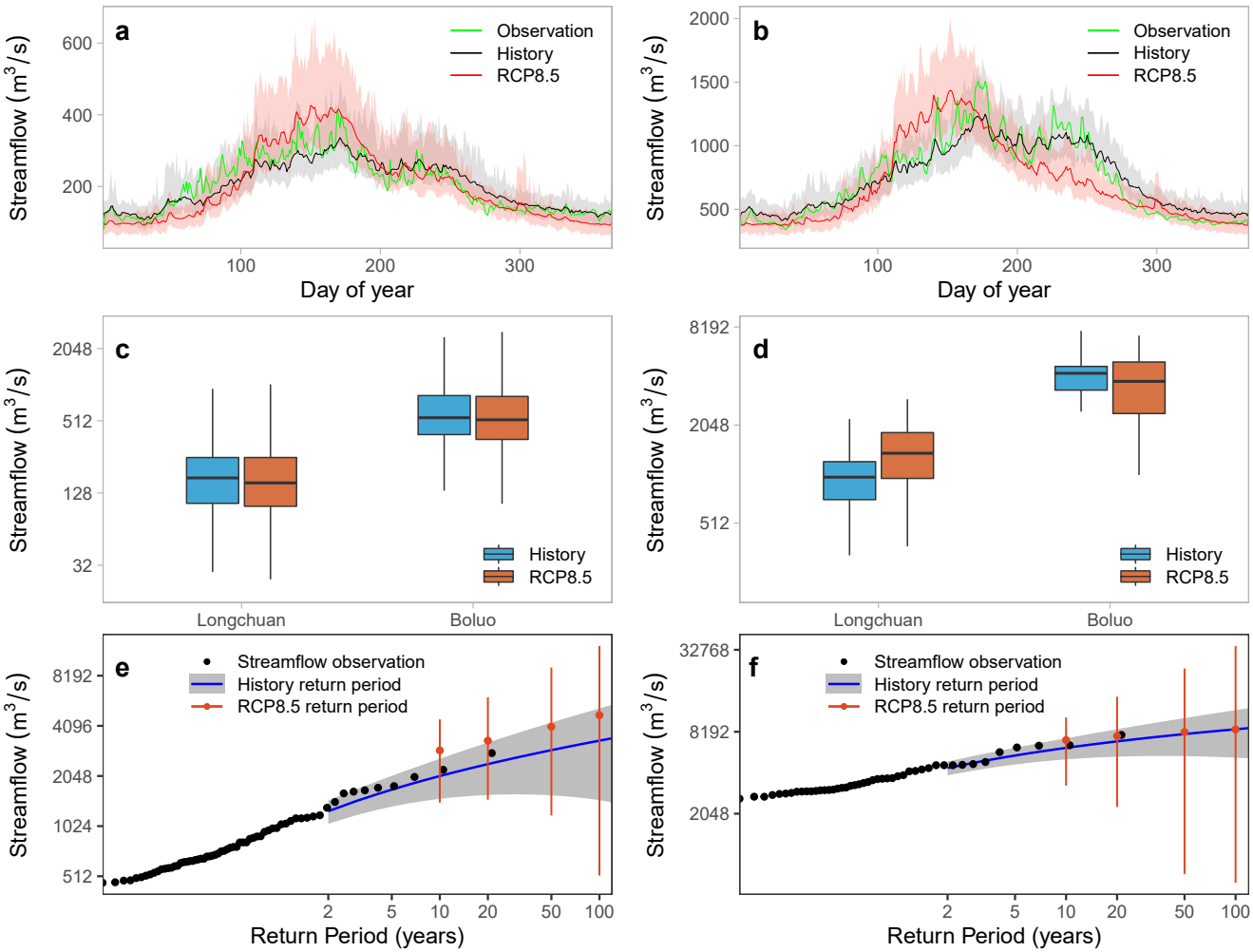

Figure 13. Comparison of streamflow regimes at present and future climates: (a) and (b) correspond to the annual cycles of streamflow over the Longchuan and Boluo stations, respectively; (c) and (d) correspond to the boxplots of daily and annual maximum streamflow, respectively; (e) and (f) correspond to the flood return levels with 95% confidence intervals estimated over the Longchuan and Boluo stations, respectively, for past and future climates. The boxplots in (c) and (d) are created with the same settings as Figure 4.

(see Figure 14c), leading to a mean contribution of up to 82%. In comparison, the model parameter contributes less to the total uncertainty than the model structure with the mean values of only 20% and 25% for the Longchuan and Boluo stations, respectively.

To further evaluate the contribution of uncertainty components to the projected change in streamflow quantiles, Figure 15 presents the variance decomposition of the changes in different streamflow quantiles over the Longchuan and Boluo stations. Results show that the model structure is an important source of uncertainty with the contribution ranging from 32% to 93% while the contribution of parameters is relatively low and varies between 4% and 45%. In particular, model structures become the dominant source of uncertainty for the high quantile range (e.g., 80%–99%), accounting for on average 84% and 65% of the total uncertainty in streamflow projections for the Longchuan and Boluo stations, respectively. Such results are consistent with those in previous studies which recognized the substantial uncertainty contribution of hydrological model structures in hydrologic simulations (Melsen et al., 2018; Van Kempen et al., 2021). The dominant contribution of model structures for the high quantile range can result from different runoff mechanisms and representation schemes of reservoir storage and operations in the SWAT and VIC models, which can be implicitly represented in the PCE models (Brunner, 2021; Duc Dang et al., 2020; Qiu et al., 2019). Therefore, neglecting model structural uncertainty can undermine the robustness of results and conclusions drawn from hydrologic projections. A multi-model

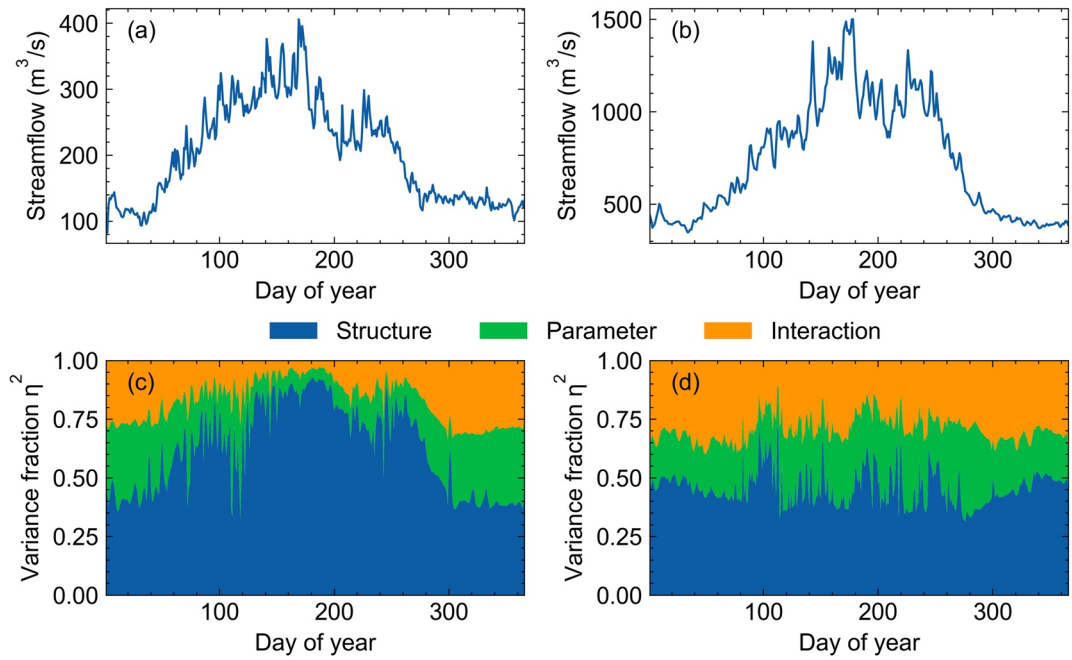

Figure 14. Variance decomposition of the uncertainty in projected mean streamflow changes at the (c) Longchuan and (d) Boluo hydrologic stations throughout the annual cycle of streamflow. (a) and (b) correspond to the annual cycles of historical streamflow for the Longchuan and Boluo hydrologic stations, respectively.

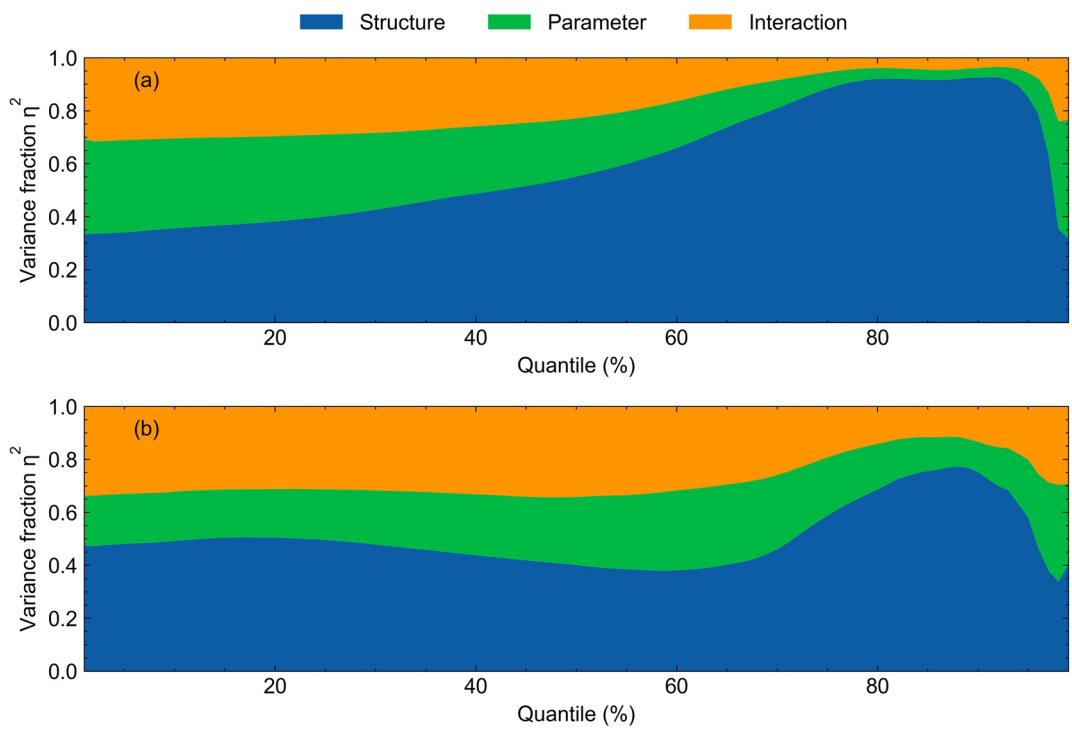

Figure 15. Variance decomposition of the uncertainty in projected changes of different streamflow quantiles for the (a) Longchuan and (b) Boluo hydrologic stations.

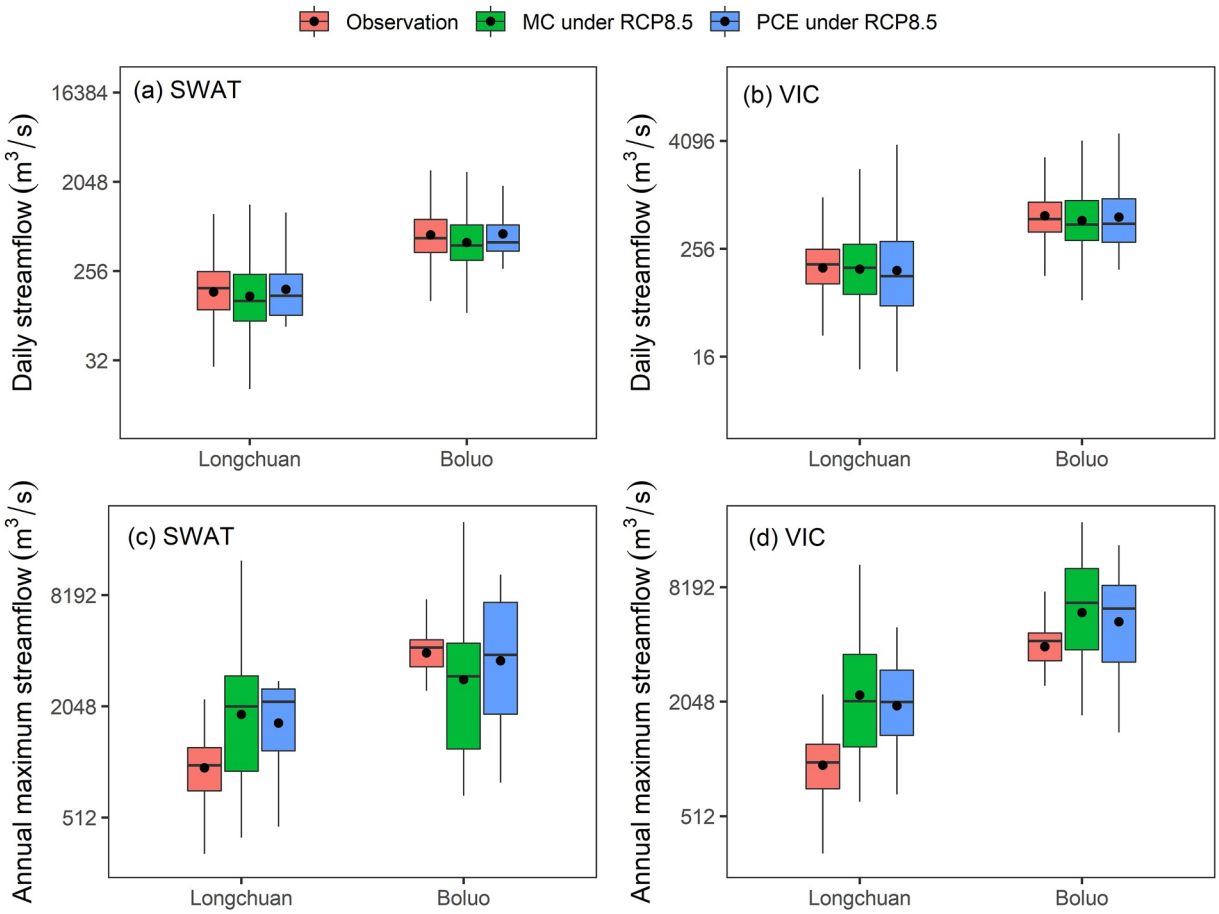

Figure 16. Comparison of streamflow regimes generated from DNN-based PCE models and hydrologic models (SWAT and VIC) at present and future climates: (a–b) and (c–d) correspond to the annual mean and maximum streamflow, respectively. MC represents Monte Carlo simulations. The boxplots are created with the same settings as Figure 4.

hydrologic projection is thus crucial for generating a reliable prediction of peak flow and flood risk (Melsen et al., 2018). The physically based multi-model hydrologic projections, however, often suffer from a considerable computational cost, which may hamper the application of multi-model techniques, especially for those large river basins. This issue can be solved using the proposed vine copula-based polynomial chaos framework, which incorporates the DNN-based PCE models and the vine copula multi-model ensemble approach into a probabilistic framework, to improve upon the physically based multi-model hydrologic projections in a computationally efficient manner.

In addition, although the DNN-based PCE model can efficiently generate plausible hydrologic predictions, it remains unclear whether such a "data-driven" approach can generate consistent future projections with physical models since the future PCE models are constructed using the DNN approach and have no physical meanings. We have performed 500 MC simulations using the SWAT and VIC models forced by the projected daily precipitation and air temperature to compare with the DNN-based PCE models. Results show that these two approaches lead to consistent future changes in the annual mean and maximum streamflow (see Figure 16), further demonstrating the reliability of the DNN-based PCE model in projecting future hydrologic regimes. The SWAT and VIC models lead to divergent future changes in the annual maximum streamflow over the Boluo station, which can be also a reason for the insignificant changes in flood magnitudes between past and future climates (Figure 13f).

5. Summary and Conclusions

In this study, we develop a vine copula-based polynomial chaos framework to improve multi-model projections of hydroclimatic regimes at a convection-permitting scale. Specifically, DNN-based PCE models are developed to improve the efficiency of probabilistic hydrologic predictions and are compared with physically based hydrologic models. A vine copula multi-model ensemble approach is also proposed to enhance the accuracy and reliability of ensemble hydrologic predictions and is compared with the existing BMA techniques. To project future changes in hydroclimatic regimes at a river basin scale, the multi-decadal climate projections are developed by using the convection-permitting WRF model with 4-km horizontal grid spacing. The proposed framework is applied to the Dongjiang River Basin located in South China for demonstrating its feasibility and applicability.

Our findings reveal that the DNN-based PCE models achieve comparable performance to the physically based models in terms of the reliability, sharpness, and accuracy of hydrologic predictions, but are more than 4,000 times faster than the physically based hydrologic models. The vine copula multi-model ensemble approach achieves higher reliability and accuracy in hydrologic predictions compared to the BMA technique. In addition, the convection-permitting climate simulations well reproduce the observed spatial patterns of historical precipitation and temperature over South China, which further increases the confidence in the projected hydrologic regimes. The projected mean precipitation and streamflow do not show obvious increases over the Dongjiang River Basin, but there will be substantial increases in the frequency and intensity of extreme precipitation. Such increases lead to the amplification of flood risks, but such amplification may not be obvious for river basins affected by multiple reservoirs. Our findings also reveal that the DNN-based PCE models and physical models lead to consistent projections of hydrologic regimes, thereby demonstrating the reliability of the proposed framework. These findings provide meaningful insights into future changes in hydroclimatic regimes over the Dongjiang River Basin, which play a crucial role in hydrologic engineering design and water resources planning in the context of climate change.

High-resolution hydroclimatic projections are subject to extensive uncertainties. In this study, we explicitly addressed the uncertainties in the structures and parameters of DNN-based PCE models and quantified the contributions of uncertainty components to the overall uncertainty in hydrologic projections. Our findings reveal that model structures are an important source of uncertainty in the projected changes of the mean annual cycle of streamflow and are the dominant source of uncertainty for peak flows. In comparison, model parameters contribute less to the overall uncertainty in climate change signals of hydrologic regimes. Thus, neglecting model structural uncertainty would undermine the robustness of results and conclusions drawn from hydrologic projections.

This study also has several limitations. The PCE technique used in this study requires the studied parameters to be independent, but it is crucial to handle the possible correlation between parameters, which can provide insights into uncertainty analysis for hydrologic models. In addition, the developed PCE models cannot be applied downstream or upstream at locations other than where they were developed, and thus it is expected to use parameter regionalization techniques to relate known physical attributes to the PCE coefficients in future studies, thereby realizing spatially distributed predictions. The DNN-based PCE model relies on the assumption that the relationship between meteorological variables and PCE coefficients remains time-invariant, which may be violated due to hydrologic nonstationarity. It is thus necessary to further improve the proposed framework to obtain probabilistic hydroclimatic projections in a nonstationary context. In addition, the vine copula-based multi-model ensemble approach fails to estimate the relative performance of each member in the ensemble such as the BMA approach. Such an approach does not generate a true prediction, but rather leads to a predictive distribution, thereby enhancing the credibility of hydrologic risk assessment. It should be also noted that the vine copula-based approach ignores serial correlation and spatial correlation in streamflow predictions generated from each model.

The recently released CMIP6 models involve more dynamic processes and have finer horizontal resolutions compared with the CMIP5 models used in this study but do not appear to reflect a substantial improvement (Agel & Barlow, 2020; J. Li et al., 2021). It remains unclear whether the CMIP6 will provide more reliable climate change signals in convection-permitting climate simulations. Thus, it is necessary to compare dynamically downscaling climate projections derived from CMIP5 and CMIP6 models in future studies.

The projected streamflow can be subject to the model bias of WRF simulations, but climate model bias is not corrected in this study due to the stationarity assumption of bias-correction approaches. Bias correction commonly relies on the hypothesis that biases from historical simulations remain the same in the future, which

cannot be tested directly since the future climate has not been realized yet. Thus, the use of bias correction may further increase the uncertainty and bring additional assumptions to hydrologic projections. Nevertheless, it is expected to examine the impacts of bias-corrected climate simulations on the projected streamflow regimes in future studies to further examine the error propagation and assumptions of hydroclimate projections.

Data Availability Statement

The MSWEP V2 precipitation product can be downloaded at http://www.gloh2o.org/mswep/. The ERA5-Land and ERA-Interim gridded reanalysis products were provided by the ECMWF, which can be obtained from the websites (https://cds.climate.copernicus.eu/cdsapp#!/dataset/reanalysis-era5-land?tab=overview and https://apps.ecmwf.int/datasets/data/interim-full-daily/levtype=sfc/). The streamflow and reservoir outflow observations were collected from the Bureau of Dongjiang River Basin Administration of Guangdong Province (http://djly.gd.gov.cn/). The WRF model outputs presented in this study can be accessed at GBAcdp (http://www.gbacdp.cn/).

Acknowledgments
This research was supported by the National Natural Science Foundation of China (Grant No. 51809223) and the Hong Kong Research Grants Council Early Career Scheme (Grant No. 25222319). The multi-decadal convection-permitting WRF simulations were performed using China's Tianhe-2 supercomputer at the National Supercomputer Center in Guangzhou. The in-situ meteorological data was provided by the National Meteorological Information Center (http://data.cma.cn/site/index.html).

References

Agel, L., & Barlow, M. (2020). How well do CMIP6 historical runs match observed Northeast U.S. precipitation and extreme precipitation–related circulation? *Journal of Climate*, *33*(22), 9835–9848. https://doi.org/10.1175/JCLI-D-19-1025.1

AghaKouchak, A., Cheng, L., Mazdiyasni, O., & Farahmand, A. (2014). Global warming and changes in risk of concurrent climate extremes: Insights from the 2014 California drought. *Geophysical Research Letters*, *41*(24), 8847–8852. https://doi.org/10.1002/2014GL062308

Anghileri, D., Voisin, N., Castelletti, A., Pianosi, F., Nijssen, B., & Lettenmaier, D. P. (2016). Value of long-term streamflow forecasts to reservoir operations for water supply in snow-dominated river catchments. *Water Resources Research*, *52*(6), 4209–4225. https://doi.org/10.1002/2015wr017864

Arnold, J. G., Srinivasan, R., Muttiah, R. S., & Williams, J. R. (1998). Large area hydrologic modeling and assessment part I: Model development. *Journal of the American Water Resources Association*, *34*(1), 73–89. https://doi.org/10.1111/j.1752-1688.1998.tb05961.x

Bass, B., & Bedient, P. (2018). Surrogate modeling of joint flood risk across coastal watersheds. *Journal of Hydrology*, *558*, 159–173. https://doi.org/10.1016/j.jhydrol.2018.01.014

Becker, T., & Wing, A. A. (2020). Understanding the extreme spread in climate sensitivity within the radiative-convective equilibrium model intercomparison project. *Journal of Advances in Modeling Earth Systems*, *12*(10). https://doi.org/10.1029/2020MS002165

Beck, H. E., Wood, E. F., Pan, M., Fisher, C. K., Miralles, D. G., Van Dijk, A. I. J. M., et al. (2019). MSWEP V2 global 3-hourly 0.1° precipitation: Methodology and quantitative assessment. *Bulletin of the American Meteorological Society*, *100*(3), 473–500. https://doi.org/10.1175/bams-d-17-0138.1

Bedford, T., & Cooke, R. M. (2002). Vines - A new graphical model for dependent random variables. *Annals of Statistics*, *30*(4), 1031–1068. https://doi.org/10.1214/aos/1031689016

Bevacqua, E., Maraun, D., Hobæk Haff, I., Widmann, M., & Vrac, M. (2017). Multivariate statistical modelling of compound events via pair-copula constructions: Analysis of floods in Ravenna (Italy). *Hydrology and Earth System Sciences*, *21*(6), 2701–2723. https://doi.org/10.5194/hess-21-2701-2017

Biondi, D., & Todini, E. (2018). Comparing hydrological postprocessors including ensemble predictions into full predictive probability distribution of streamflow. *Water Resources Research*, *54*(12), 9860–9882. https://doi.org/10.1029/2017WR022432

Blum, A. G., Archfield, S. A., & Vogel, R. M. (2017). On the probability distribution of daily streamflow in the United States. *Hydrology and Earth System Sciences*, *21*(6), 3093–3103. https://doi.org/10.5194/hess-21-3093-2017

Bohn, T. J., Sonessa, M. Y., & Lettenmaier, D. P. (2010). Seasonal hydrologic forecasting: Do multimodel ensemble averages always yield improvements in forecast skill? *Journal of Hydrometeorology*, *11*(6), 1358–1372. https://doi.org/10.1175/2010JHM1267.1

Bosshard, T., Carambia, M., Goergen, K., Kotlarski, S., Krahe, P., Zappa, M., & Schär, C. (2013). Quantifying uncertainty sources in an ensemble of hydrological climate-impact projections. *Water Resources Research*, *49*(3), 1523–1536. https://doi.org/10.1029/2011WR011533

Brunner, M. I. (2021). Reservoir regulation affects droughts and floods at local and regional scales. *Environmental Research Letters*, *16*(12), 124016. https://doi.org/10.1088/1748-9326/AC36F6

Brunner, M. I., Papalexiou, S., Clark, M. P., & Gilleland, E. (2020). How probable is widespread flooding in the United States? *Water Resources Research*, *56*(10), e2020WR028096. https://doi.org/10.1029/2020WR028096

Chen, L., & Frauenfeld, O. W. (2014). A comprehensive evaluation of precipitation simulations over China based on CMIP5 multimodel ensemble projections. *Journal of Geophysical Research: Atmospheres*, *119*(10), 5767–5786. https://doi.org/10.1002/2013JD021190

Dai, C., Xue, L., Zhang, D., & Guadagnini, A. (2016). Data-worth analysis through probabilistic collocation-based ensemble Kalman filter. *Journal of Hydrology*, *540*, 488–503. https://doi.org/10.1016/j.jhydrol.2016.06.037

Dee, D. P., Uppala, S. M., Simmons, A. J., Berrisford, P., Poli, P., Kobayashi, S., et al. (2011). The ERA-Interim reanalysis: Configuration and performance of the data assimilation system. *Quarterly Journal of the Royal Meteorological Society*, *137*(656), 553–597. https://doi.org/10.1002/qj.828

Dißmann, J., Brechmann, E. C., Czado, C., & Kurowicka, D. (2013). Selecting and estimating regular vine copulae and application to financial returns. *Computational Statistics & Data Analysis*, *59*(1), 52–69. https://doi.org/10.1016/j.csda.2012.08.010

Duan, Q., Ajami, N. K., Gao, X., & Sorooshian, S. (2007). Multi-model ensemble hydrologic prediction using Bayesian model averaging. *Advances in Water Resources*, *30*(5), 1371–1386. https://doi.org/10.1016/j.advwatres.2006.11.014

Duc Dang, T., Kamal Chowdhury, A. F. M., & Galelli, S. (2020). On the representation of water reservoir storage and operations in large-scale hydrological models: Implications on model parameterization and climate change impact assessments. *Hydrology and Earth System Sciences*, *24*(1), 397–416. https://doi.org/10.5194/hess-24-397-2020

Evin, G., Thyer, M., Kavetski, D., McInerney, D., & Kuczera, G. (2014). Comparison of joint versus postprocessor approaches for hydrological uncertainty estimation accounting for error autocorrelation and heteroscedasticity. *Water Resources Research*, *50*(3), 2350–2375. https://doi.org/10.1002/2013WR014185

Fan, Y. R., Huang, G. H., Baetz, B. W., Li, Y. P., Huang, K., Li, Z., et al. (2016). Parameter uncertainty and temporal dynamics of sensitivity for hydrologic models: A hybrid sequential data assimilation and probabilistic collocation method. *Environmental Modelling & Software*, *86*, 30–49. https://doi.org/10.1016/j.envsoft.2016.09.012

Ghaith, M., & Li, Z. (2020). Propagation of parameter uncertainty in SWAT: A probabilistic forecasting method based on polynomial chaos expansion and machine learning. *Journal of Hydrology*, *586*, 124854. https://doi.org/10.1016/j.jhydrol.2020.124854

Giorgi, F. (2019). Thirty years of regional climate modeling: Where are we and where are we going next? *Journal of Geophysical Research: Atmospheres*, *124*(11), 5696–5723. https://doi.org/10.1029/2018JD030094

Gonçalves, R. C., Iskandarani, M., Srinivasan, A., Thacker, W. C., Chassignet, E., & Knio, O. M. (2016). A framework to quantify uncertainty in simulations of oil transport in the ocean. *Journal of Geophysical Research: Oceans*, *121*(4), 2058–2077. https://doi.org/10.1002/2015JC011311

Gou, J., Miao, C., Duan, Q., Tang, Q., Di, Z., Liao, W., et al. (2020). Sensitivity analysis-based automatic parameter calibration of the VIC model for streamflow simulations over China. *Water Resources Research*, *56*(1), e2019WR025968. https://doi.org/10.1029/2019WR025968

Gruber, L. F., & Czado, C. (2018). Bayesian model selection of regular vine copulas. *Bayesian Analysis*, *13*(4), 1107–1131. https://doi.org/10.1214/17-BA1089

Gudmundsson, L., Boulange, J., Do, H. X., Gosling, S. N., Grillakis, M. G., Koutroulis, A. G., et al. (2021). Globally observed trends in mean and extreme river flow attributed to climate change. *Science*, *371*(6534), 1159–1162. https://doi.org/10.1126/science.aba3996

Hersbach, H. (2000). Decomposition of the continuous ranked probability score for ensemble prediction systems. *Weather and Forecasting*, *15*(5), 559–570. https://doi.org/10.1175/1520-0434(2000)015<0559:DOTCRP>2.0.CO;2

Hersbach, H., Bell, B., Berrisford, P., Hirahara, S., Horányi, A., Muñoz-Sabater, J., et al. (2020). The ERA5 global reanalysis. *Quarterly Journal of the Royal Meteorological Society*, *146*(730), 1999–2049. https://doi.org/10.1002/qj.3803

Hu, J., Chen, S., Behrangi, A., & Yuan, H. (2019). Parametric uncertainty assessment in hydrological modeling using the generalized polynomial chaos expansion. *Journal of Hydrology*, *579*, 124158. https://doi.org/10.1016/j.jhydrol.2019.124158

Isukapalli, S. S. (1999). *Uncertainty analysis of transport-transformation models*. Rutgers The State University of New Jersey-New Brunswick.

Jiang, Z., Li, W., Xu, J., & Li, L. (2015). Extreme precipitation indices over China in CMIP5 models. Part I: Model evaluation. *Journal of Climate*, *28*(21), 8603–8619. https://doi.org/10.1175/JCLI-D-15-0099.1

Jing, X., Geerts, B., Wang, Y., & Liu, C. (2019). Ambient factors controlling the wintertime precipitation distribution across mountain ranges in the interior Western United States. Part II: Changes in orographic precipitation distribution in a pseudo-global warming simulation. *Journal of Applied Meteorology and Climatology*, *58*(4), 695–715. https://doi.org/10.1175/JAMC-D-18-0173.1

Knoben, W. J. M., Freer, J. E., Peel, M. C., Fowler, K. J. A., & Woods, R. A. (2020). A brief analysis of conceptual model structure uncertainty using 36 models and 559 catchments. *Water Resources Research*, *56*(9). https://doi.org/10.1029/2019WR025975

Kollet, S., Sulis, M., Maxwell, R. M., Paniconi, C., Putti, M., Bertoldi, G., et al. (2017). The integrated hydrologic model intercomparison project, IH-MIP2: A second set of benchmark results to diagnose integrated hydrology and feedbacks. *Water Resources Research*, *53*(1), 867–890. https://doi.org/10.1002/2016WR019191

Krysanova, V., Vetter, T., Eisner, S., Huang, S., Pechlivanidis, I., Strauch, M., et al. (2017). Intercomparison of regional-scale hydrological models and climate change impacts projected for 12 large river basins worldwide - A synthesis. *Environmental Research Letters*, *12*(10), 86105002. https://doi.org/10.1088/1748-9326/aa8359

Kurkute, S., Li, Z., Li, Y., & Huo, F. (2020). Assessment and projection of the water budget over Western Canada using convection-permitting weather research and forecasting simulations. *Hydrology and Earth System Sciences*, *24*(7), 3677–3697. https://doi.org/10.5194/hess-24-3677-2020

Laloy, E., Rogiers, B., Vrugt, J. A., Mallants, D., & Jacques, D. (2013). Efficient posterior exploration of a high-dimensional groundwater model from two-stage Markov chain Monte Carlo simulation and polynomial chaos expansion. *Water Resources Research*, *49*(5), 2664–2682. https://doi.org/10.1002/wrcr.20226

Li, H., & Zhang, D. (2007). Probabilistic collocation method for flow in porous media: Comparisons with other stochastic methods. *Water Resources Research*, *43*(9). https://doi.org/10.1029/2006WR005673

Li, J., Huo, R., Chen, H., Zhao, Y., & Zhao, T. (2021). Comparative assessment and future prediction using CMIP6 and CMIP5 for annual precipitation and extreme precipitation simulation. *Frontiers of Earth Science*, *9*, 430. https://doi.org/10.3389/FEART.2021.687976/BIBTEX

Li, W., & Sankarasubramanian, A. (2012). Reducing hydrologic model uncertainty in monthly streamflow predictions using multimodel combination. *Water Resources Research*, *48*(12). https://doi.org/10.1029/2011WR011380

Li, Y., Li, Z., Zhang, Z., Chen, L., Kurkute, S., Scaff, L., & Pan, X. (2019). High-resolution regional climate modeling and projection over Western Canada using a weather research forecasting model with a pseudo-global warming approach. *Hydrology and Earth System Sciences*, *23*(11), 4635–4659. https://doi.org/10.5194/hess-23-4635-2019

Liang, X., Lettenmaier, D. P., Wood, E. F., & Burges, S. J. (1994). A simple hydrologically based model of land surface water and energy fluxes for general circulation models. *Journal of Geophysical Research*, *99*(D7). https://doi.org/10.1029/94jd00483

Liao, Q., & Zhang, D. (2016). Probabilistic collocation method for strongly nonlinear problems: 3. Transform by time. *Water Resources Research*, *52*(3), 2366–2375. https://doi.org/10.1002/2015WR017724

Lin, G., & Tartakovsky, A. M. (2009). An efficient, high-order probabilistic collocation method on sparse grids for three-dimensional flow and solute transport in randomly heterogeneous porous media. *Advances in Water Resources*, *32*(5), 712–722. https://doi.org/10.1016/j.advwatres.2008.09.003

Liu, Z., Cheng, L., Hao, Z., Li, J., Thorstensen, A., & Gao, H. (2018). A Framework for exploring joint effects of conditional factors on compound floods. *Water Resources Research*, *54*(4), 2681–2696. https://doi.org/10.1002/2017WR021662

Madadgar, S., & Moradkhani, H. (2014). Improved Bayesian multimodeling: Integration of copulas and Bayesian model averaging. *Water Resources Research*, *50*(12), 9586–9603. https://doi.org/10.1002/2014WR015965

Maina, F. Z., & Siirila-Woodburn, E. R. (2020). The role of subsurface flow on evapotranspiration: A global sensitivity analysis. *Water Resources Research*, *56*(7), 1–20. https://doi.org/10.1029/2019WR026612

Man, J., Zheng, Q., Wu, L., & Zeng, L. (2019). Improving parameter estimation with an efficient sequential probabilistic collocation-based optimal design method. *Journal of Hydrology*, *569*, 1–11. https://doi.org/10.1016/j.jhydrol.2018.11.056

Melsen, L. A., Addor, N., Mizukami, N., Newman, A. J., Torfs, P. J. J. F., Clark, M. P., et al. (2018). Mapping (dis)agreement in hydrologic projections. *Hydrology and Earth System Sciences*, *22*(3), 1775–1791. https://doi.org/10.5194/hess-22-1775-2018

Moradkhani, H., Hsu, K. L., Gupta, H., & Sorooshian, S. (2005). Uncertainty assessment of hydrologic model states and parameters: Sequential data assimilation using the particle filter. *Water Resources Research*, *41*(5), 1–17. https://doi.org/10.1029/2004WR003604

Musselman, K. N., Lehner, F., Ikeda, K., Clark, M. P., Prein, A. F., Liu, C., et al. (2018). Projected increases and shifts in rain-on-snow flood risk over Western North America. *Nature Climate Change*. https://doi.org/10.1038/s41558-018-0236-4

Olson, R., Fan, Y., & Evans, J. P. (2016). A simple method for Bayesian model averaging of regional climate model projections: Application to southeast Australian temperatures. *Geophysical Research Letters*, *43*(14), 7661–7669. https://doi.org/10.1002/2016GL069704

Prein, A. F., Rasmussen, R., & Stephens, G. (2017). Challenges and advances in convection-permitting climate modeling. *Bulletin of the American Meteorological Society*, *98*(5), 1027–1030. https://doi.org/10.1175/BAMS-D-16-0263.1

Qing, Y., & Wang, S. (2021). Multi-decadal convection-permitting climate projections for China's Greater Bay Area and surroundings. *Climate Dynamics*. https://doi.org/10.1007/s00382-021-05716-w

Qing, Y., Wang, S., Ancell, B. C., & Yang, Z.-L. (2022). Accelerating flash droughts induced by the joint influence of soil moisture depletion and atmospheric aridity. *Nature Communications*, *13*, 1139. https://doi.org/10.1038/s41467-022-28752-4

Qiu, J., Yang, Q., Zhang, X., Huang, M., Adam, J. C., & Malek, K. (2019). Implications of water management representations for watershed hydrologic modeling in the Yakima River basin. *Hydrology and Earth System Sciences*, *23*(1), 35–49. https://doi.org/10.5194/hess-23-35-2019

Raftery, A. E., Gneiting, T., Balabdaoui, F., & Polakowski, M. (2005). Using Bayesian model averaging to calibrate forecast ensembles. *Monthly Weather Review*, *133*(5), 1155–1174. https://doi.org/10.1175/MWR2906.1

Razavi, S., Tolson, B. A., & Burn, D. H. (2012). Review of surrogate modeling in water resources. *Water Resources Research*, *48*(7), 7401. https://doi.org/10.1029/2011WR011527

Sadegh, M., Ragno, E., & AghaKouchak, A. (2017). Multivariate copula analysis toolbox (MvCAT): Describing dependence and underlying uncertainty using a Bayesian framework. *Water Resources Research*, *53*(6), 5166–5183. https://doi.org/10.1002/2016WR020242

Sharma, S., Siddique, R., Reed, S., Ahnert, P., & Mejia, A. (2019). Hydrological model diversity enhances streamflow forecast skill at short-to medium-range timescales. *Water Resources Research*, *55*(2), 1510–1530. https://doi.org/10.1029/2018WR023197

Sun, C., Huang, G., Fan, Y., Zhou, X., Lu, C., & Wang, X. (2021). Vine copula ensemble downscaling for precipitation projection over the Loess Plateau based on high-resolution multi-RCM outputs. *Water Resources Research*, *57*(1), 2020WR0698. https://doi.org/10.1029/2020WR027698

Sun, X., Tu, Q., Chen, J., Zhang, C., & Duan, X. (2018). Probabilistic load flow calculation based on sparse polynomial chaos expansion. *IET Generation, Transmission & Distribution*, *12*(11), 2735–2744. https://doi.org/10.1049/iet-gtd.2017.0859

Thyer, M., Renard, B., Kavetski, D., Kuczera, G., Franks, S. W., & Srikanthan, S. (2009). Critical evaluation of parameter consistency and predictive uncertainty in hydrological modeling: A case study using Bayesian total error analysis. *Water Resources Research*, *45*(12), W00B14. https://doi.org/10.1029/2008WR006825

Torre, E., Marelli, S., Embrechts, P., & Sudret, B. (2019). A general framework for data-driven uncertainty quantification under complex input dependencies using vine copulas. *Probabilistic Engineering Mechanics*, *55*, 1–16. https://doi.org/10.1016/j.probengmech.2018.08.001

Tran, V. N., Dwelle, M. C., Sargsyan, K., Ivanov, V. Y., & Kim, J. (2020). A novel modeling framework for computationally efficient and accurate real-time ensemble flood forecasting with uncertainty quantification. *Water Resources Research*, *56*(3), 1–31. https://doi.org/10.1029/2019WR025727

Van Kempen, G., Van Der Wiel, K., & Anna Melsen, L. (2021). The impact of hydrological model structure on the simulation of extreme runoff events. *Natural Hazards and Earth System Sciences*, *21*(3), 961–976. https://doi.org/10.5194/NHESS-21-961-2021

Viana, F. A. C., Gogu, C., & Goel, T. (2021). Surrogate modeling: Tricks that endured the test of time and some recent developments. *Structural and Multidisciplinary Optimization*, *64*(5), 2881–2908. https://doi.org/10.1007/s00158-021-03001-2

Vrugt, J. A. (2016). Markov chain Monte Carlo simulation using the DREAM software package: Theory, concepts, and MATLAB implementation. *Environmental Modelling & Software*, *75*, 273–316. https://doi.org/10.1016/j.envsoft.2015.08.013

Vrugt, J. A., & Robinson, B. A. (2007). Treatment of uncertainty using ensemble methods: Comparison of sequential data assimilation and Bayesian model averaging. *Water Resources Research*, *43*(1), 1–15. https://doi.org/10.1029/2005WR004838

Wang, H., Gong, W., Duan, Q., & Di, Z. (2020). Evaluation of parameter interaction effect of hydrological models using the sparse polynomial chaos (SPC) method. *Environmental Modelling & Software*, *125*, 104612. https://doi.org/10.1016/j.envsoft.2019.104612

Wang, S., Ancell, B. C., Huang, G. H., & Baetz, B. W. (2018). Improving robustness of hydrologic ensemble predictions through probabilistic pre- and post-processing in sequential data assimilation. *Water Resources Research*, *54*(3), 2129–2151. https://doi.org/10.1002/2018WR022546

Wang, S., & Wang, Y. (2019). Improving probabilistic hydroclimatic projections through high-resolution convection-permitting climate modeling and Markov chain Monte Carlo simulations. *Climate Dynamics*, *53*(3–4), 1613–1636. https://doi.org/10.1007/s00382-019-04702-7

Wiener, N. (1938). The homogeneous chaos. *American Journal of Mathematics*, *60*(4), 897. https://doi.org/10.2307/2371268

Yan, Z., Zhou, Z., Liu, J., Han, Z., Gao, G., & Jiang, X. (2020). Ensemble projection of runoff in a large-scale basin: Modeling with a global BMA approach. *Water Resources Research*, *56*(7), e2019WR026134. https://doi.org/10.1029/2019WR026134

You, J., & Wang, S. (2021). Higher probability of occurrence of hotter and shorter heat waves followed by heavy rainfall. *Geophysical Research Letters*, *48*(17), e2021GL094831. https://doi.org/10.1029/2021GL094831

Zhang, B., & Wang, S. (2021). Probabilistic characterization of extreme storm surges induced by tropical cyclones. *Journal of Geophysical Research: Atmospheres*, *126*(3), e2020JD033557. https://doi.org/10.1029/2020JD033557

Zhang, B., Wang, S., & Wang, Y. (2019). Copula-based convection-permitting projections of future changes in multivariate drought characteristics. *Journal of Geophysical Research: Atmospheres*, *124*(14), 7460–7483. https://doi.org/10.1029/2019JD030686

Zhang, B., Wang, S., & Wang, Y. (2021). Probabilistic projections of multidimensional flood risks at a convection-permitting scale. *Water Resources Research*, *57*(1), e2020WR028582. https://doi.org/10.1029/2020WR028582

Zhang, J., Zheng, Q., Chen, D., Wu, L., & Zeng, L. (2020). Surrogate-based Bayesian inverse modeling of the hydrological system: An adaptive approach considering surrogate approximation error. *Water Resources Research*, *56*(1), 1–25. https://doi.org/10.1029/2019WR025721

Zhu, J., Wang, S., & Huang, G. (2019). Assessing climate change impacts on human-perceived temperature extremes and underlying uncertainties. *Journal of Geophysical Research: Atmospheres*, *124*(7), 3800–3821. https://doi.org/10.1029/2018JD029444

Zscheischler, J., Martius, O., Westra, S., Bevacqua, E., Raymond, C., Horton, R. M., et al. (2020). A typology of compound weather and climate events. *Nature Reviews Earth & Environment*, *1*(7), 333–347. https://doi.org/10.1038/s43017-020-0060-z